2020-08

Synthesis, Characterization and Assessment of Antibacterial Activity of Novel Homobinuclear Mixed Ligand Copper (Ii) Complexes Containing Resorcinol ate, Acetone and Ethylene Demine.

Misganaw, Tegegne

BAHIR DAR UNIVERSITY

COLLEGE OF SCIENCE

POSTGRADUATE PROGRAM

DEPARTMENT OF CHEMISTRY

A THESIS ON:

SYNTHESIS, CHARACTERIZATION AND ASSESMENT OF ANTIBACTERIAL ACTIVITY OF NOVEL HOMOBINUCLEAR MIXED LIGAND COPPER (II) COMPLEXES CONTAINNING RESORCINOLATE, ACETONE AND ETHYLENE DIAMINE.

BY: MISGANAW TEGEGNE AYANA

ADVISORS: BELETE BEDEMO (PhD, Associate professor) AND

ATAKILT ABEBE (PhD, Associate professor)

AUGUT, 2020

BAHIR DAR, ETHIOPIA

APPROVAL SHEET

The thesis entitled synthesis, characterization and assessment of antibacterial activity of novel homobinuclear mixed ligand copper (II) complexes containing resorcinolate, acetone and ethylenediamine.

Submitted by:

Misganaw Tegegne Ayana _____ _____

Signature Date

This thesis submitted to post graduate program, Chemistry department to the partial fulfillment of the requirement for the degree of Master of science in chemistry (organic chmistry), Bahir Dar University done by Misganaw Tegegne under our supervision is sufficient to full fill the requirement. Being the examiner of this thesis, it is sufficient to full fill the requirement.

Approved by:

Name of Advisors:

Belete Bedemo (PhD) _____ _____

Signature Date

Atakilt Abebe (PhD) _____ _____

Signature Date

Name of Internal Examiners:

1._____ _____ _____

Signature Date

2. _____ _____ _____

Signature Date

Name of External Examiner:

_____ _____ _____

Signature Date

ACKNOWLEDGMENT

My sincere gratitude goes to my Advisors, Dr. Belete Bedemo and Dr. Atakilt Abebe for their immense contributions, guidance, constructive criticism, innovative ideas, encouragement and brotherly approach during the whole course of this research including financial support. To be honest, without my advisors help and guidance, this thesis would not have been successful. Equivalently, I would like to acknowledge Dr. Getinet Tamiru for his valuable suggestions, advices, guidance, and encouragement throughout this work.

Next, I would like to acknowledge all staff members of organic chemistry stream for their multi-dimensional support. My deepest gratitude also extends to Dr. Maereg Amare and his research group for their willingness and contribution to run cyclic voltammetry. And I want to thank department of Chemistry, college of science, Bahir dar University to give this chance and prepare different accesses to do this research.

Additionally, I would like to thank department of Biology(Microbiology) college of science, Bahir dar University. Finally, my heartfelt gratitude never forgotten for my family especially for my mother and my sister to their priceless effort to grow me with good behavior and for their multidimensional support up to this end.

Table CONTENTS

LIST OF FIGURES

LIST OF SCHEMES

LIST OF TABLES

LIST OF APPENDICES

LIST OF ABBREVIATIONS AND ACRONYMS

ATCC	American type culture collection
BM	Bohr magneton
CV	Cyclicvoltametry
DCM	Dichloromethane
DMSO	Dimethyl Sulphoxide
DNA	Deoxyribonucleic acid
EtOAc	Ethyl acetate
E.Coil	Escherichia coli
FT-IR	Fourier transform Infrared
ICP-OES	Inductively coupled Plasma Optical Emission Spectroscopy
K.pneumonia	Klebsiella Pneumonia
LMCT	Metal to ligand charge transfer
MIC	Minimum inhibitory concentration
MLCT	Ligand to metal charge transfer
MRSA	Methicillin-Resistant Staphylococcus Aureus
ppm	Parts per million
S.aureus	Staphyloccus aureus
S. Pyogenes	Streptococcus pyogens
TGA	Thermal gravimetric analysis
THF	Tetrahydrofuran
TLC	Thin Layer Chromatography
UV-Vis	Ultraviolate- visible
VRE	Vancomycin Resistant Enterococci

ABSTRACT

Transition metal complexes are endowed with properties suitable for inhibition of bacterial infectious diseases. Based on this, identification and synthesis of new transition metal complexes is a passion for scientists. In this report copper (II) homobinuclear mixed ligand complexes containing resorcinolate (R), acetone (Ac) and ethylenediamine (en) with formula $H_4[Cu_2(R^{2-})_2(R^-)_4]$, $H_4[Cu_2(R^{2-})_2(R^-)_4Ac_2]$, $H_8[Cu_2(R^{2-})_6en]$, $H_8[Cu_2(R^{2-})_6en_2]$, $H_4[Cu_2(R^{2-})_2(R^-)_4enAc]$, *and* $Na_8[Cu_2(R^{2-})_6]$ *were synthesized. The structures of the synthesized complexes were characterized using various analytical, electrochemical and spectroscopic techniques, particularly using UV-Vis, FT-IR, ICP-OES, CV, Molar conductivity, pH, Melting point, Qualitative chloride test and Solubility tests. Furthermore, the synthesized complexes were evaluated for their in vitro antibacterial activities against some Gram-positive (Staphyloccus aureus and Streptococcus pyogens) and Gram-negative (Escherichia coli, Klebsiella Pneumonia) bacterial species by disc diffusion method and the result obtained were compared with the commercially available drug gentamicin by calculating percent activity index. The complexes were found to be active against all the tested bacteria. According to the percent activity index data, most complexes have higher antibacterial activity than gentamicin even in gram-negative bacterial strains. So, after the in vivo cytotoxicity investigation, pre-clinical and clinical tests the newly synthesized complexes could be considered as potential antimicrobial agent.*

Keywords: Synthesis, characterization, resorcinolate, ethylenediamine, acetone, Cu (II) homobinuclear mixed ligand complex and antibacterial activity.

1. INTRODUCTION

1.1. Background of the study

The large percentage of use and misuse of antibiotics led to a serious public health problems due to bacterial resistance to antibiotics [**1, 2**]. Most infections are caused by bacteria such as methicillin-resistant Staphylococcus aureus (MRSA), vancomycin resistant enterococci (VRE), Escherichia coli, Klebsiella pneumoniae, etc. Despite the large number of antibiotics available for medical use, parallel emergence of old and new antibiotic resistance demanded for new classes of antimicrobial agents with new mode of action. [**3**].

Transition metal mixed ligand complexes show a wide range of applications including pharmacology, toxicology and biochemistry. Thus, suitable coordination environments with spectral and electrochemical properties of the complexes results effective interactions with DNA [**4, 5**]. Particularly, copper (II) complexes of mixed-ligands are of great interest since they exhibit numerous biological activities. Copper is a bioimpact element with two biologically accessible oxidation states. There are reports indicating its mixed-ligand complexes bring about oxidative and electrolytic cleavage of DNA [**4**].

Binuclear complexes have attracted considerable attention leading to their application in many areas of modern medicine. For example, mixed ligand binuclear copper (II) complex of 5-methyl salicyl aldehyde and 2,2-bipyridyl $[Cu(MS)(bpy)]_2.(ClO_4)_2$ have been investigated for their DNA binding and nuclease activities. The result indicated a good binding propensity and bind to nitrogenous bases of DNA by intercalation. The crystal structure of the complex shows that copper (II) ion lies in a square pyramidal coordination environment [**4**]. Furthermore, mono and binuclear copper (II) complexes of hydrazone ligands derived from 4,6-diacetylresorcinol, nitrogen-donor ligands such as 1,10-phenanthroline and pentamethyl diethylenetriamine as well as thiodiglycolate anion $[(HL^1)Cu(OAc)(H_2O)].1.5H_2O$ and $[(L^2)Cu_2(OAc)_2(Phen)_2]\_3H_2O$ $C_5 4H_4 6N_{10}O_{11}Cu_2]$ have been investigated for their antimicrobial activities. Moreover, a novel mixed-ligand complexes of Cu (II) metal containing 1,10-phenanthroline and thymine have $[Cu(L_1)_2(H_2O)_2]Cl_2$ and $[Cu(L_1)_2L_2H_2O]Cl$ (L_1 = 1,10phenanthroline, L_2 = thymine) been prepared, characterized and subjected to antibacterial test for different bacterial strains[**6-8**].

In all cases, significant improvements in their biological activities have been observed. Nevertheless, all these research findings revealed that, still change in the compositions of the metal ion with various unexplored ligands may result in new complexes with a set of new properties and applications. Owing to this, literature survey indicated a gap that the study of homobinuclear mixed ligand complexes of Cu (II) using resorcinol, acetone and ethylenediamine as ligand found to be necessary.

Resorcinol has been used for about 100 years in human medicine as an antiseptic and in keratolytic topical medications in low concentrations of 1–2%. Sometimes much higher concentrations (up to 50%) have been used in peeling agents or in pastes for the treatment of leg ulcers. Dihydroxybenzenes have two hydroxyl groups available for coordination to metal ions. So it can act as monodentate or bidentate ligand [**9, 23**]. Additionally, alkyl resorcinol and aromatic resorcinol are reported to possess valuable therapeutic and antiseptic properties. Basically, 4-alkyl resorcinol is reported to have skin beautifying effect, low toxicity and irritation when applied on to human skin [**10**].

Ethylenediamine forms a large number of complexes with many different metal ions. It acts as a monodentate, chelating as well as bridging ligand [**11**].

1.2. Statement of the problem

The resistance of microbes to the current commercially available drugs is a problem of the medical and pharmaceutical industries. So, it is important to develop novel drugs with a new mode of action which targets the lipid layer of the microbes and their life cycle **[12, 13]**. Recently, transition metal complexes have been a focus of attention. Particularly, a number of copper (II) complexes used in therapeutic applications were reported [**14**]. However, there is no report on the chemistry of copper (II) based homobinuclear mixed ligand complex containing resorcinolate, acetone and ethylelendiamine. So, this study attempts to focus on synthesis, characterization and assess the antibacterial activity of such complexes.

1.3. Significance of the study

Recently, the increasing of life threatening infectious diseases caused by multi-drug resistant pathogens is an alarming rate. Based on this, pharmaceutical industries are looking for synthesizing alternative compounds to medicinal preparations originating from wild growing plants. However, plant based drugs have shortened the life span of the source. To alleviate these problems, synthesis and investigations of different metal complexes have been carried out and

promising results are being found. The actions of these complexes against the microbes were reported to be *via* non covalent interactions with the DNA. The significance of this project is, therefore, complementing the effort of discovering new complexes containing different ligands having different features with new mode of actions.

1.4. Objectives of the study

1.4.1. General objective

To synthesize characterization and evaluate the antibacterial activities of copper (II) homobinuclear mixed ligand complexes containing resorcinolate, ethylenediamime and acetone.

1.4.2. Specific objectives

- ☞ To synthesize homobinuclear Cu (II) complexes from $CuCl_2$ salt, resorcinol, acetone and ethylenediamine with different compositions as follow:
    - ✓ From $CuCl_2$ salt and resorcinol in 1:3 mole ratio.
    - ✓ From the first homobinuclear complex and ethylenediamine in 1: 2 mole ratio.
    - ✓ From the first homobinuclear complex and ethylenediamine in 1:1 mole ratio.
    - ✓ From the first homobinuclear complex and acetone in 1: 1 mole ratio.
    - ✓ From the homobinuclear complex containing acetone and ethylenediamine in 1:1 mole ratio.
    - ✓ From $CuCl_2.2H_2O$ salt and resorcinol in 1:3 mole ratio by using strong base as deprotonating agent.
- ☞ To characterize the synthesized complexes using various analytical, electrochemical and spectroscopic techniques.
- ☞ To investigate the antibacterial activities of the synthesized complexes against Gram positive and Gram negative bacteria.
- ☞ To compare the antibacterial activities of Cu (II) complexes with commercially available drugs.

2. LITERATURE REVIEW

2.1. Coordination chemistry and mixed ligand complexes

Coordination chemistry is about tuning properties of metal ions using different ligands [**15**]. Based on this, synthesis of different coordination compounds with desired properties by ligand tailoring has become a fascinating research field. Designing new coordination compounds with therapeutic abilities has been part of this activity [**16**].

The concepts of mixed ligand complexes are always fascinating to the chemistry community. Consequently, interest in synthesis of mixed ligand complexes is rising. This is because; these complexes contained at least two different kinds of ligands with different properties associated with the same metal ion. The combined effect of the ligands with different properties on the metal ion in a complex results in a set of new properties. This includes stabilization of different oxidation states and modulation of the solvophilicity, electrophilic and nucleophilic properties of the metal ion and the ligands. While coordinating, the properties of the ligands themselves are also modified [**17, 18**].

2.2. Overview of the chemistry of Cu (II) Complexes and ligands

2.2.1. Chemistry of Cu (II) complexes

Copper in trace quantities is required by all living organisms to maintain proper cellular functions. A great majority of Cu (II) compounds are blue or green in color because of a single broad absorption band in the region of 600-900nm which is due to spin allowed transition $^2T_{2g} \rightarrow {}^2E_g$. Considerable distortion in octahedral symmetry is observed in Cu (II) complexes. The magnetic moment of mononuclear Cu (II) complexes are generally in the range of 1.75-2.20 BM, regardless of stereochemistry and independent of temperature except at extremely low temperature [**19**]. Copper (II) forms stable complexes with nitrogen and oxygen donor ligands. Cu (II) complexes of nitrogen ligands are generally stable. The most common coordination numbers of Cu (II) are 4, 5 and 6 with square-planar, square pyramidal and octahedral geometries, respectively.

Binuclear copper (II) complexes have an important functional role in many metalloenzymes. An important example is catechol oxidase. It catalyzes the oxidation of O-diphenol to the corresponding O-quinone coupled with $2e/2H^+$ reduction of O_2 to H_2O. The structure of catechol oxidase (figure 1) contains binuclear copper (II) centers in which each copper (II) is coordinated

to three histidine nitrogen atoms followed by an exogenous bridging hydroxide group forming a four coordinated trigonal pyramidal geometry. Thus, the copper (II) species using binuclear complex forming ligands have attracted increasing attention in recent years [**20**].

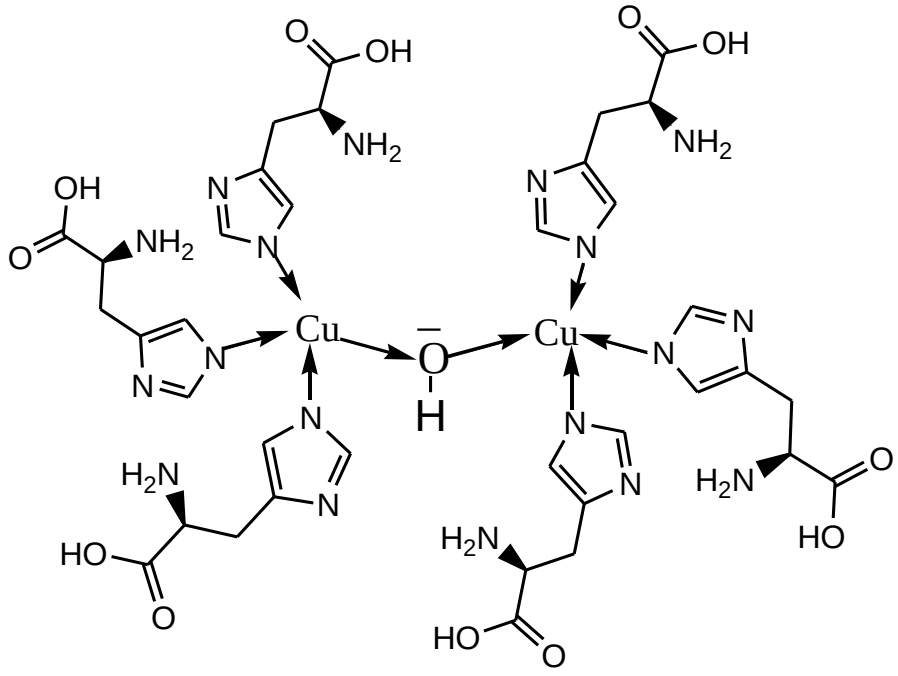

Figure 1: Structure of catechol oxidase isolated from sweet potato [**20**].

2.2.2. Chemistry of resorcinol and its application

Resorcinol molecule has two hydroxyl groups in the aromatic ring structure, and they are located at meta-positions with respect to each other Figure 2. The high reactivity of resorcinol is primarily associated with the location of these two hydroxyl groups in the benzene ring. As far as the reactivity of resorcinol is concerned, the hydrogen atom adjacent to the hydroxyl groups, namely at carbon atoms 2, 4 and 6 are particularly reactive towards electrophilic substitution. All these three positions of the molecules are doubly activated by the two hydroxyl groups. Electrophilic substitution reaction such as alkylation, acylation, halogenation, nitration and sulfonation can occur predominantly [**21**].

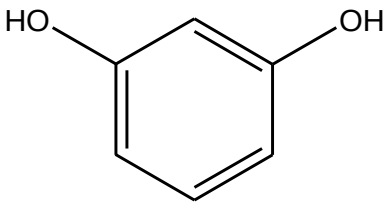

Figure 2: Structure of Resorcinol

It is used as a chemical intermediate in manufacturing of pharmaceuticals, dyestuffs and fungicides such as P-amino salicylic acid, hexylresorcinol and light screening agents for protecting plastics from UV lights [**22**]. It has a melting point of 111 ^{0}C and used in the formulation of several pharmaceuticals such as acne creams, hair dyes, anti-dandruff shampoos, and sun tan lotions. It also possesses various therapeutic uses such as topical antipruritic and antiseptic. It is used to treat seborrhea dermatitis, psoriasis, corns, warts and eczema. It is effective in the treatment of several dermatological problems due to its antibacterial, antifungal and keratolytic effects. Resorcinol solution in ethyl alcohol (Jessner's solution) is used in chemical peeling and it has special medical use as biological glue (gelatin-resorcinol-formaldehyde glue) in cardiovascular surgery [**23**]. Dihydroxybenzenes have two hydroxyl groups available for coordination to metal ions [**24**]. So, it can act as monodentate or bidentate ligand. There are studies on determination of formation constant of resorcinol complexes with different metal ions. For example, the binary and ternary complexes of some transition metal ions with resorcinol as primary ligand for the determination of formation constants of complexes [**9**].

2.2.3. Chemistry of ethylenediamine and its properties

Ethylenediamine is colorless molecule at room temperature having the characteristic smell of an amine. It has a melting point of 11.1 ^{0}C and a boiling point of 116.9 ^{0}C at 101325 Pa (1 atm.). With time the composition tends to change, especially in the presence of air. It absorbs both water and carbon dioxide from the atmosphere forming the carbonate, and it forms a stable monohydrate which can be distilled without decomposition, but fractional distillation does not normally lead to a very pure product. Ethylenediamine forms a large number of complexes with many different metal ions. It usually acts as a bidentate ligand and examples are known in which ethylenediamine acts either as a monodentate or a bridging ligand Figure 3. But, in a few rare cases, ethylenediamine form a monoprotonated complexes [**11**].

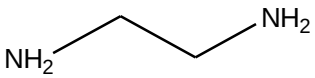

Figure 3: Structure of Ethylenediamine

2.2.4. Chemistry of acetone and its application in coordination chemistry

Acetone (propanone) is the simplest and smallest ketone Figure 4. It is a colorless, volatile, flammable liquid with a characteristic odor. Acetone is miscible with water and serves as an important solvent in its own right, in industry, home, and laboratory [**25**]. It is a common building block in organic chemistry. Familiar household uses of acetone are as the active ingredient in nail polish remover and as paint thinner. Acetone is produced and disposed of in the human body through normal metabolic processes. It is normally present in blood and urine. People with diabetes produce it in larger amounts [**26**]. A series of complexes were reported acetone as the ligand in which it is a weakly coordinating ligand. Complexes of acetone (hexa-solvated cations) with divalent metals such as Mg(II), Ca(II), Mn(II), Fe(II), Co(II), and Ni(II) forms octahedral complex by solvation[**27**]. Usually, acetone reacts with Lewis acids to give adducts. [**28, 29**]

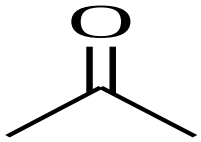

Figure 4: Structure of Acetone

2.3. Overview on synthesis, structural investigation and Biological activity of some mononuclear and binuclear Cu (II) complexes with different ligands

A number of mono and binuclear copper (II) complexes have been reported. For instance, four complexes by slight variation of (2E)-2-(2-hydroxy-3-methoxybenzylidene)-4N-substituted hydrazine carbothioamides, $(OH)(OCH_3)C_6H_4CH=NNHC(S)NHR$, where R=H ($L_1$), Me ($L_2$), Et ($L_3$), or Ph ($L_4$), $[Cu_2(L_1)_2Cl_2]$, $[Cu_2(L_2)_2Cl_2]$, $[Cu_2(L_3)_2Cl_2]$ and $[Cu_2(L_4)_2Cl_2]$ have been synthesized and characterized both the ligands and complexes were tested for antibacterial activities by agar disc diffusion method. Except for complex 4, all complexes showed

considerable activity almost equal to the activity of ciprofloxacin. These complexes did not show any effect on Gram-negative bacteria, whereas they showed moderate activity for Gram-positive strains [**30**].

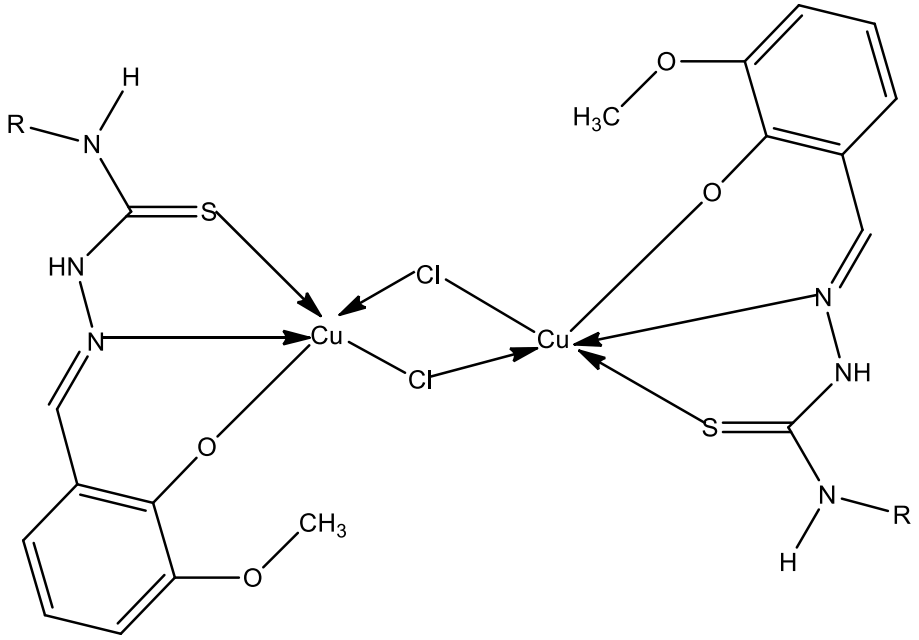

Where R = H, $\mathbf{L}_1$

= CH_3, $\mathbf{L}_2$

= C_2H_5, $\mathbf{L}_3$

= C_6H_5, $\mathbf{L}_4$

Figure 5: Structure of Cu (II) (2E)-2-(2-hydroxy-3-methoxybenzylidene)-4N-substituted hydrazine carbothioamides complexes [**30**].

Furthermore, mixed ligand complexes of Cu (II) metal containing 1,10-phenanthroline and thymine $[Cu(L_1)_2(H_2O)_2]Cl_2$ and $[Cu(L_1)_2L_2H_2O]Cl$ (L_1 = 1,10-phenanthroline, L_2 = thymine) have been prepared, characterized and the antibacterial activities against Staphylococcus aureus, Streptococcus pneumonia, methicillin-resistant Staphylococcus aureus (MRSA), Klebsiella pneumoniae, Escherichia coli and Shigella boydii was studied. The biological activities of the complexes showed enhanced antimicrobial activity compared to the free metal salt with thymine being lower than that of 1,10-phenanthroline. [**8**].

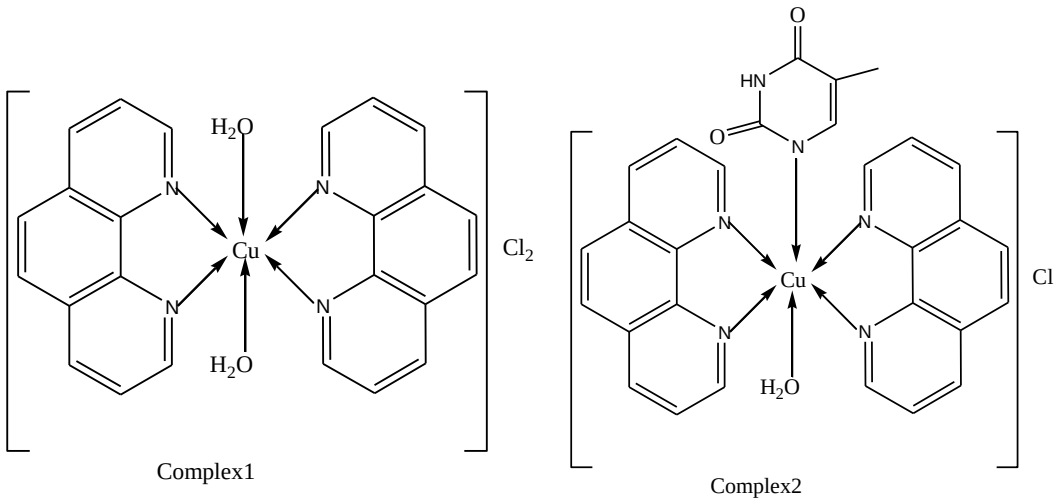

Figure 6: Structure of Cu (II) 1,10-phenanthroline (Complex1) and Cu (II) 1,10-phenanthroline mixed with thymine (Complex2) [**8**].

2.4. Mechanism of action of antimicrobial agents

Most Cu (II) complexes showed promising biological activities and this was supported by the DNA binding affinity of the Cu (II) complexes which was postulated to be due to the ability of the complexes to block the enzymatic binding to the nitrogen bases of DNA or RNA of the cancer cells [**31**]. Several other copper complexes have been reported to have effective anti-inflammatory, antirheumatic and anticancer activities, which was associated with their superoxide dismutase-like activity [**22**]. In addition, copper is also part of the redox active metalloenzymes which consists of cytochrome c oxidase and tyrosinase [**32**]. Once the complex passed the cell membrane/wall, the labile ligands separates from the complex leaving coordination sites. This phenomenon created a convenient condition for the complex to act as a carrier agent that delivers active ligands *in vivo*. This resulted in independent interactions of these fragments with the pathogenic cell [**8**]. Based on this we anticipated that, the synthesized complexes will have better activity *in vivo.* Regardless of the large number of reports, there is still the need of preparation of Cu (II) complexes with better activities due to new modes of actions against the pathogen cells. In this regard, the search for new metal complexes bearing labile ligands which may coordinate with the disease targets through ligand exchange reaction with biomolecules is sought. Thus we synthesized new homobinuclear Copper (II) complexes with a proposed formula: $H_4[Cu_2(R^{2-})_2(R^-)_4]$, $H_4[Cu_2(R^{2-})_2(R^-)_4Ac_2]$, $H_8[Cu_2(R^{2-})_6en]$, $H_8[Cu_2(R^{2-})_6en_2]$, $H_4[Cu_2(R^{2-})_2(R^-)_4enAc]$, and $Na_8[Cu_2(R^{2-})_6]$ respectively.

3. MATERIALS AND METHODS

In this study, synthesis of homobinuclear mixed ligand complexes containing Cu (II) metal, resorcinolate, acetone and etheylenediamine were prepared in stepwise manner under optimized reaction conditions. The complexes were synthesized by a method with a slight modification of a method used in 3, 8 and16. The complexes were characterized using various analytical, electrochemical and spectroscopic techniques. Finally, there antibacterial activity study with some gram positive and gram negative bacteria was carried out.

3.1. Materials

3.1.1. Chemicals and reagents

The chemicals and solvents that were used in this study: $CuCl_2.2H_2O$ salt (PhilipHaeris, Limited, England), resorcinol (Himedialaboratory,pvt,ltd,India), ethylenediamine, $AgNO_3$ (Blulux Laboratories(P),ltd-121 001), Na_2SO_4 (Blulux Laboratories (p) ltd.-121 001), HNO_3(65%, Lobachemie), $HClO_4$(60%, Sisco), H_2SO_4 (98%,Lobachemie), KBr (Blulux Laboratories (p) ltd.-121 001), solvents like Distilled water, methanol (India) Pvt. Ltd.), ethanol (Himedialaboratory, pvt,ltd,India), acetone (Germen, Dutch, Polish), acetonitrile (India,Pvt,Ltd.), dichloromethane (UN1593), THF(Anhui Royal chemical Co., Ltd.), ethyl acetate (Lobachemie) and diethyl ether (Tokyo chemical industry UK Ltd.) were of analytical reagent grade and used without further purification.

3.1.2. Instruments and apparatus

The necessary apparatus and instruments used for this study were digital balance(OHAUS),(hot plate, round bottom flask, burette, pan, magnetic stirrer) for reflux set up, vacuum rotary evaporator set up, (Sanyo SP65) UV-Vis spectrophotometer, (Perkin Elmer BX) FT-IR spectrophotometer, (PerkinElmer Optima 8000V) ICP-OES spectrometer, Potentiostat (CHI360E), (Stuart SMP30) digital Melting point apparatus, digital conductivity meter (BANTE901P), digital pH meter (BANTE901P), volumetric flask, beaker, Whateman No.1 filter paper, micropipette and others were used.

3.2. Methods

3.2.1. Synthetic protocols of metal complexes

3.2.1.1. Synthesis of Bi-μ–Resorcinoxobi (diresorcinol cupprate(II)) acid $H_4[Cu_2(R^{2-})_2(R^-)_4]$

The coordinated water in $CuCl_2.2H_2O$ was removed first by heating at 150 ^{0}C in an oven. And brown colored ($CuCl_2$) salt was obtained. Then, added to a 30 mL of THF solution of $CuCl_2$(1.22 g, 9.0 mmol) in a 250 mL round bottomed flask magnetically stirred in water bath at room temperature, 30 mL THF solution of resorcinol (3.62 g, 27.0 mmol) was added drop wise from a burette. The stirring continued for 3h at room temperature after the last drop of ligand solution. The reaction progress was monitored by color change and TLC. A greenish homogeneous solution was formed. The solvent was removed by rotary evaporator and a reddish brown hygroscopic solid was obtained (yield 2.26 g, 88.4%).The synthesis strategy is indicated in scheme 1. Hence, the moles described in the scheme are in simple whole number ratio.

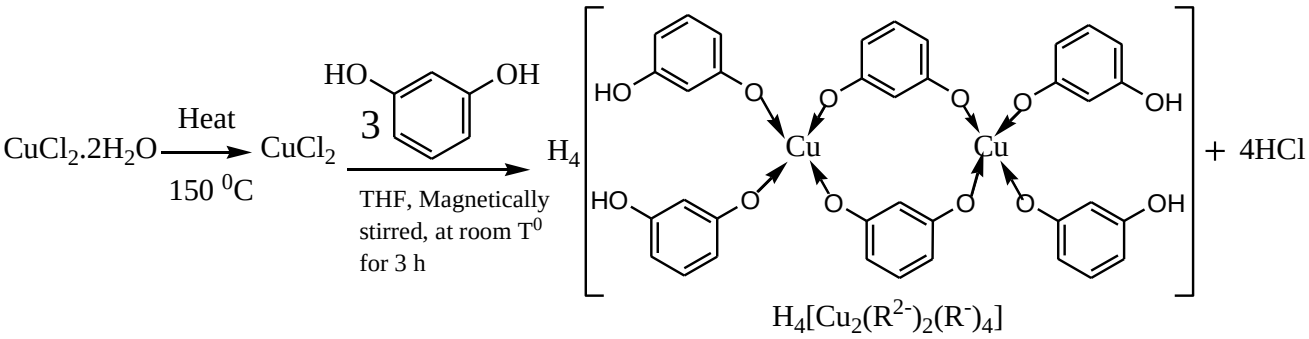

Scheme 1: Synthetic path of $H_4[Cu_2(R^{2-})_2(R^-)_4]$.

3.2.1.2. Synthesis of Bi-μ–Resorcinoxobi(aeetonediresorcinolcupprate(II)) acid $H_4[Cu_2(R^{2-})_2(R^-)_4Ac_2]$

$H_4[Cu_2(R^{2-})_2(R^-)_4Ac_2]$was formed by tandem addition of excess acetone to $H_4[Cu_2(R^{2-})_2(R^-)_4]$ complex (1.12 g, 4.06 mmol). While continuously stirred magnetically in a water bath for 30 min at room temperature, a reddish brown homogenous solution was obtained. Then the solution was concentrated by rotary evaporator. After rotary evaporator a plum color powder was obtained (yield 1.54 g, 85.6%).The synthesis strategy is indicated in scheme 2.

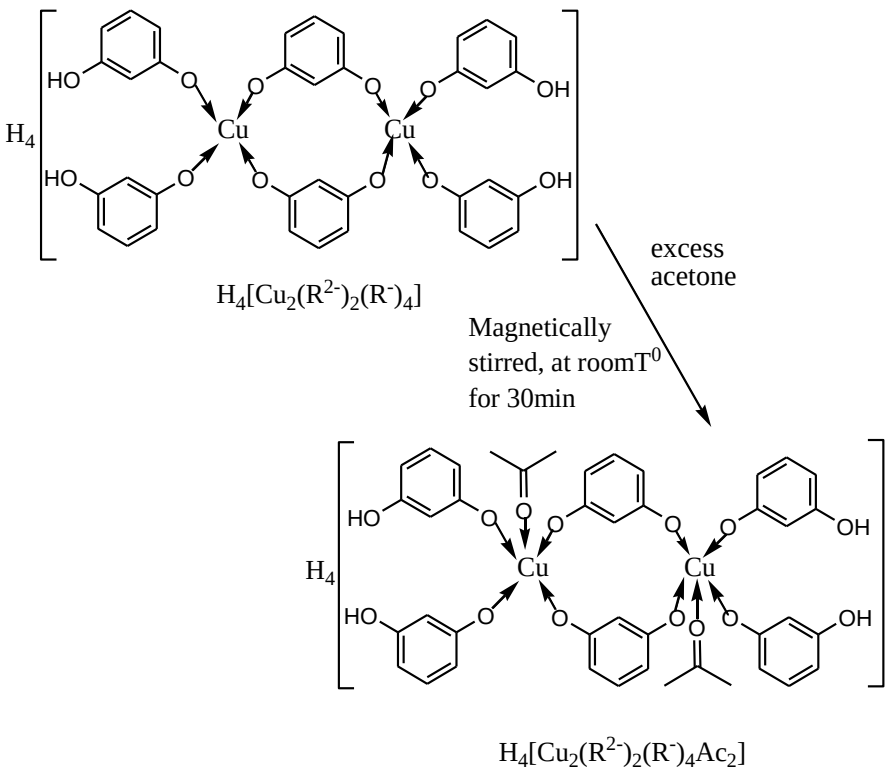

Scheme 2: Synthetic path of $H_4[Cu_2(R^{2-})_2(R^-)_4Ac_2]$.

3.2.1.3. Synthesis of Bi-μ–Resorcinoxoacetoneethylenediamine bi(diresorcinolcupprate(II)) acid $H_4[Cu_2(R^{2-})_2(R^-)_4enAc]$

$H_4[Cu_2(R^{2-})_2(R^-)_4enAc]$ was prepared by drop wise addition of a solution ethylenediamine (55µl, 0.81mmol) in 30 mL THF from a burette to a solution of $H_4[Cu_2(R^{2-})_2(R^-)_4Ac_2]$ (0.72 g, 0.80mmol) in 30 mL of THF in a 250 mL round bottom flask while continuously stirred magnetically in a water bath for 2 h at room temperature. The reaction progress was monitored by color change and TLC. Later on a brown homogenous solution was obtained. Then the solvent was removed by rotary evaporator. After rotary evaporator a maroon color gummy solid was obtained (yield 0.5 g, 86.2%).The synthesis strategy is indicated in scheme 3.

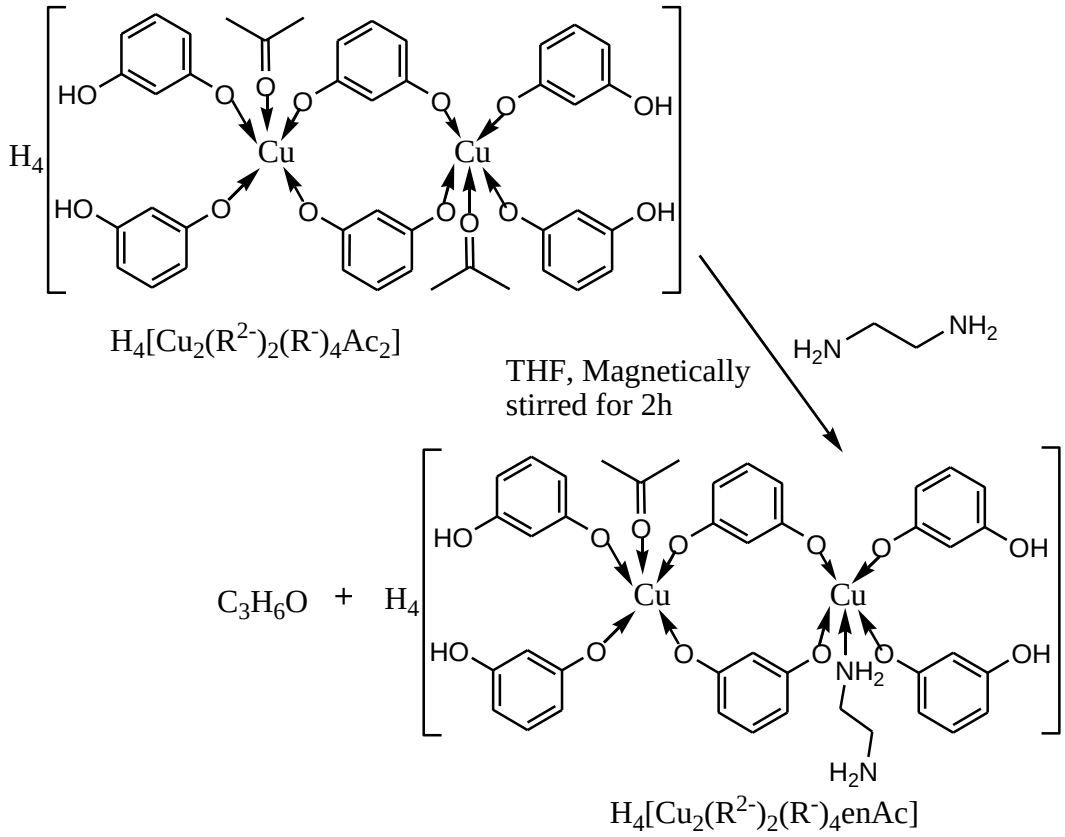

Scheme 3: Synthetic path of $H_4[Cu_2(R^{2-})_2(R^-)_4enAc]$.

3.2.1.4. Synthesis of Bi-μ–Resorcinoxobi(ethylenediaminediresorcinolate cupprate(II)) acid $H_8[Cu_2(R^{2-})_6en_2]$

$H_8[Cu_2(R^{2-})_6en_2]$ was prepared by drop wise addition of a solution of etylenediamine (545 µL, 8 mmol) in 30 mL THF from a burette to a solution of $H_4[Cu_2(R^{2-})_2(R^-)_4]$ (1.24 g, 1.6 mmol) in 30 ml of THF in a 250 mL round bottom flask while continuously stirred magnetically in a water bath for 2 h at room temperature. The reaction progress was monitored by color change and TLC. Later on a yellow precipitate was formed and after filtration a greenish brown homogenous solution was obtained. Then the solvent was removed by rotary evaporator. After rotary evaporator a saddle brown color hygroscopic solid was obtained (yield 1.15 gm, 82.7%). The synthesis strategy is indicated in scheme 4.

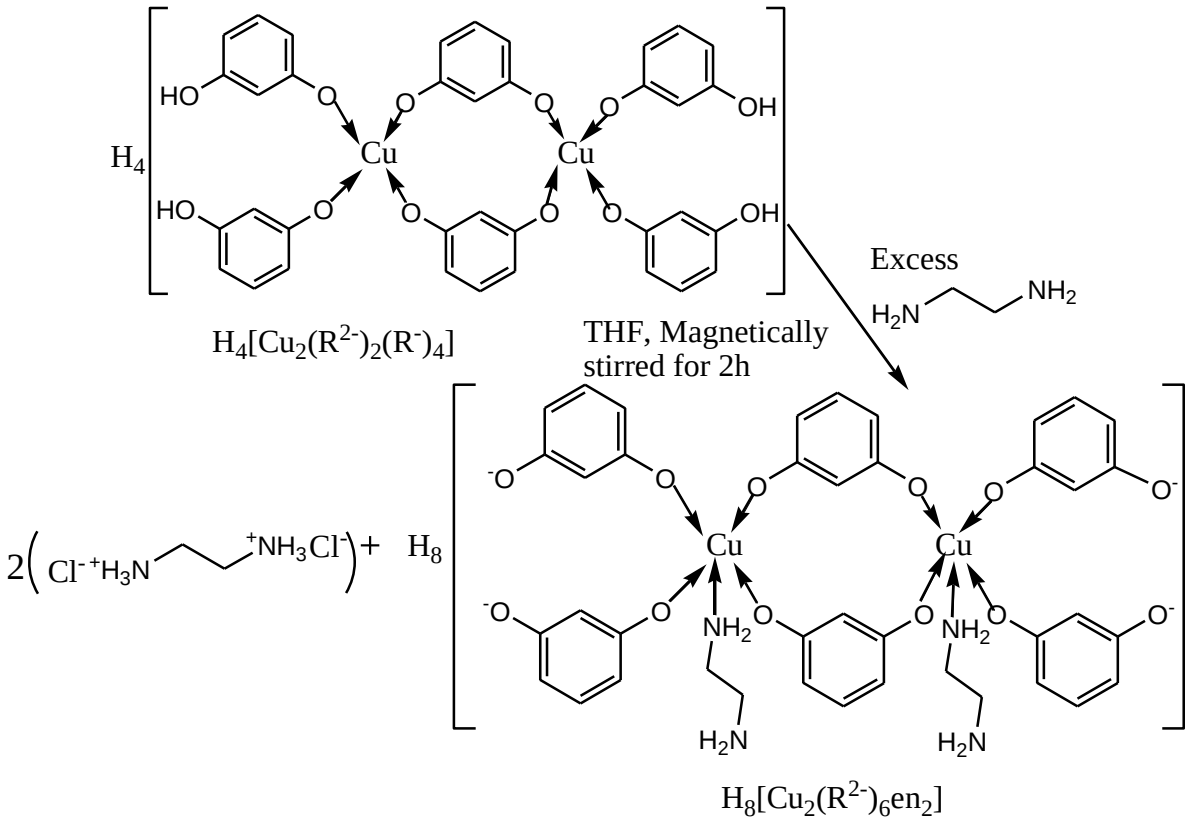

Scheme 4: Synthetic path of $H_8[Cu_2(R^{2-})_6en_2]$.

3.2.1.5. Synthesis of Bi-μ–Resorcinoxo-μ–ethylenediaminebi (diresorcinolate cupprate(II)) acid $H_8[Cu_2(R^{2-})_6en]$

$H_8[Cu_2(R^{2-})_6en]$ was prepared by drop wise addition of a solution of en (295μL, 4.4 mmol) in 30 mL THF from a burette to a solution of $H_4[Cu_2(R^{2-})_2(R^-)_4]$ (1.22 g, 1.5 mmol) in 30 mL of THF in a 250 mL round bottom flask while continuously stirred magnetically in a water bath for 3 h at room temperature. The reaction progress was monitored by color change and TLC. Later on a yellow precipitate was formed and after filtration a greenish brown homogenous solution was obtained. Then the solvent was removed by rotary evaporator. After rotary evaporator a pink color hygroscopic solid was obtained (yield 1.12 g, 83%).The synthesis strategy is indicated in scheme 5.

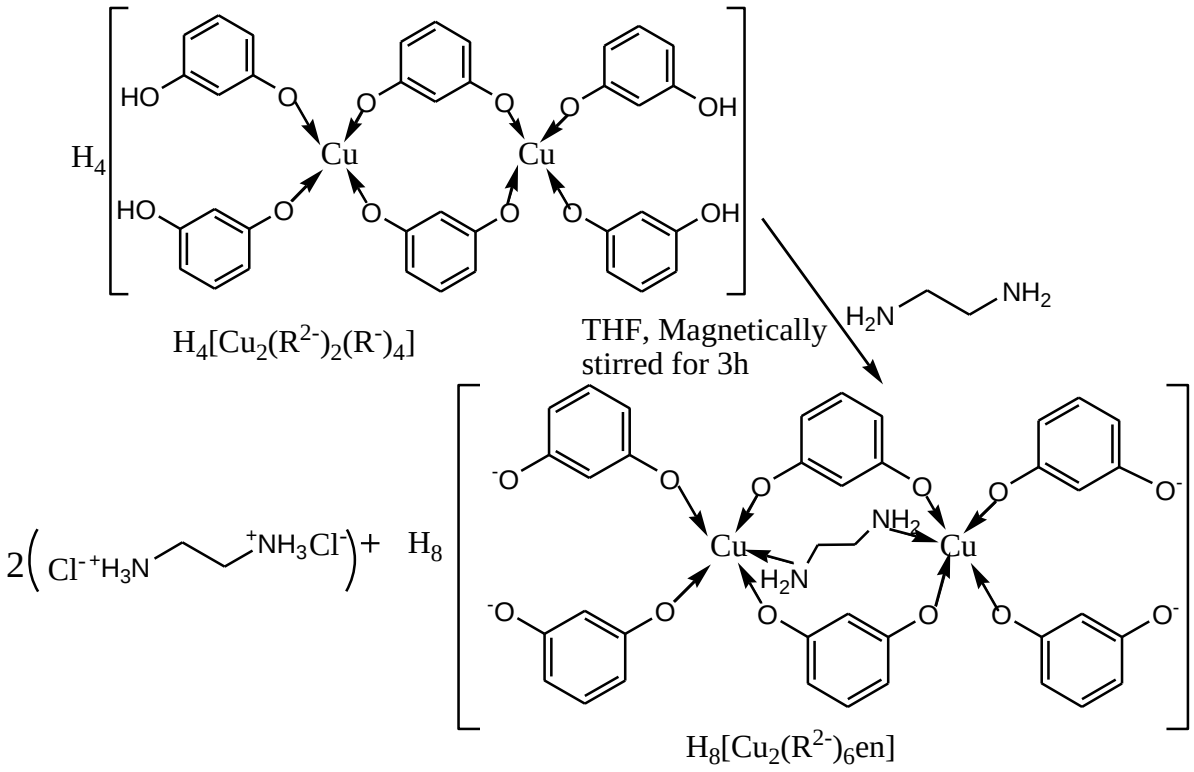

Scheme 5: Synthetic path of $H_8[Cu_2(R^{2-})_6en]$.

3.2.1.6. Synthesis of Sodium bi-μ–Resorcinoxobi(diresorcinolate cupprate(II)) $Na_8[Cu_2(R^{2-})_6]$

3.2.1.6.1. Deprotonation of resorcinol (Formation of Sodium resorcinolate)

Sodium resorcinolate was prepared by the treatment of resorcinol with 0. 456 M NaOH. A (2.5 g, 22.8 mmol) of resorcinol was dissolved in 15 mL of distilled water followed by drop wise addition of NaOH (1.824 g, 45.6 mmol) in 50 mL distilled water from a burette to a solution of resorcinol. While, the solution was stirred magnetically and titrate for 1 h the colorless solution was changed to green color**.**

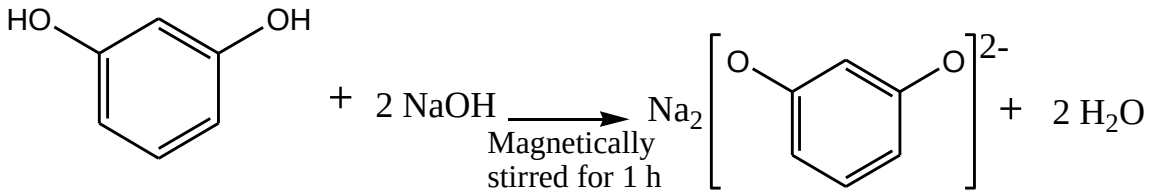

Scheme 6: Synthetic path of Sodium resorcinolate.

3.2.1.6.2. Coordination of resorcinolate to Cu (II) metal

$Na_8[Cu_2(R^{2-})_6]$ was prepared by drop wise addition of a solution of Sodium resorcinolate in H_2O from a burette to a solution of $CuCl_2.2H_2O$ (1.3 g, 7.6 mmol) in 15 mL of H_2O in a 250 mL round bottom flask and continuously stirred magnetically in a water bath for 3 h at room temperature. Later on a white colloid was obtained. After 15 h, a white precipitate was settled and the precipitate was filtered. The remaining byproduct (NaCl) was removed by dissolving with ethanol because NaCl is not soluble in ethanol. Then the solution was filtered and the solvent was removed by rotary evaporator. After rotary evaporator a wine color hygroscopic solid was obtained (yield 2.12 g, 85.5%).The synthesis strategy is indicated in scheme 7.

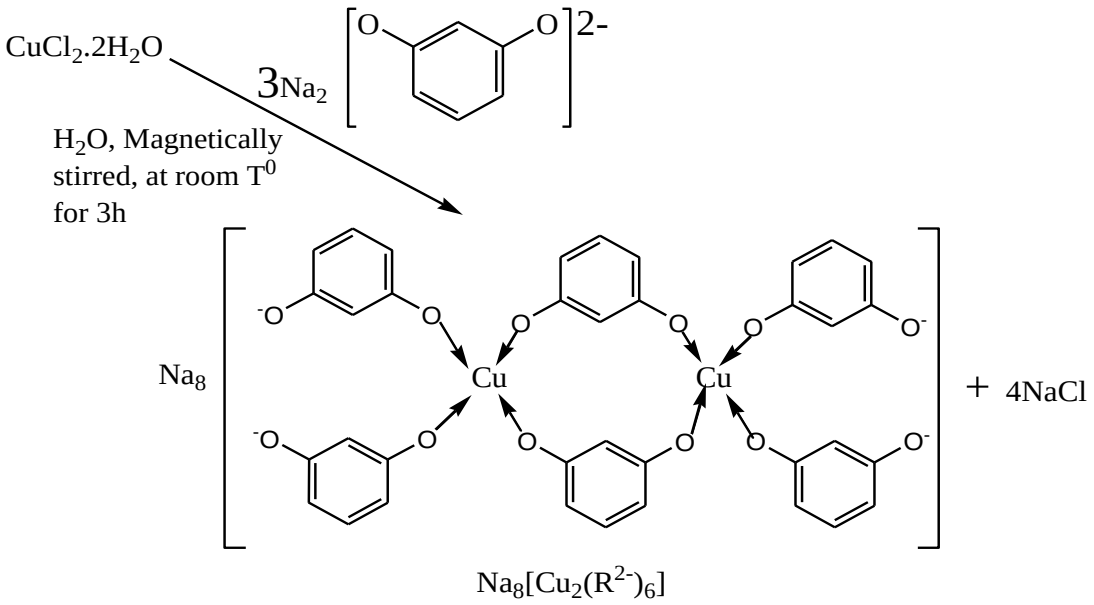

Scheme 7: Synthetic path of $Na_8[Cu_2(R^{2-})_6]$.

3.2.2. Characterization of metal complexes

3.2.2.1. Physicochemical characterizations

3.2.2.1.1. Solubility test

The solubility of the synthesized complexes was determined by using some polar and non-polar solvents.

3.2.2.1.2. Color and melting /decomposition temperature determination

The color of each metal complex was detected by the visual observation and compared with color charts. Melting points of the synthesized complexes were determined by taking small amount of complexes in one side opened capillary tube and introduced in to the opened pores of the apparatus. Then the temperature was noted when the metal complexes were first get melted or decomposed.

3.2.2.1.3. Qualitative chloride test

Qualitative chloride tests for the complexes were done by dissolving 0.003 g of the complexes and excess amount of $AgNO_3$solution were added to the solution of complexes in separate small beakers.

3.2.2.1.4. pH measurement

The pH of the complexes in water and ethanol for ($H_4[Cu_2(R^{2-})_2(R^-)_4Ac_2]$ and $H_4[Cu_2(R^{2-})_2(R^-)_4enAc$**]**) solution was measured by using digital pH meter (BANTE901P). The apparatus was first calibrated by standard buffer solution. Then the electrode was dipped in solutions of the complexes and the reading was recorded after it stabilizes.

3.2.2.1.5. Molar conductivity measurement

The molar conductivity of the complexes were determined in water and ethanol for ($H_4[Cu_2(R^{2-})_2(R^-)_4Ac_2]$ and $H_4[Cu_2(R^{2-})_2(R^-)_4enAc]$). Taking 1×10^{-3} M concentration of each complex at room temperature measure by using digital conductivity meter (BANTE901P). The conductivity meter was first calibrated by calibrants. Then the electrode was dipped in each complex solution and the reading was recorded after it stabilizes. The molar conductance was determined from conductivity measurements of the complexes.

3.2.2.2.Spectroscopic techniques

3.2.2.2.1. Metal determination / ICP-OES measurement

Quantitative analysis of copper(II) ion of the complexes were done using PerkinElmer, Optima 8000 VHF ICP-OES spectrometer, by digesting $H_4[Cu_2(R^{2-})_2(R^-)_4]$(26.8 mg), $H_8[Cu_2(R^{2-})_6en_2]$(22.5 mg), $H_8[Cu_2(R^{2-})_6en]$ (21.1 mg), $H_4[Cu_2(R^{2-})_2(R^-)_4Ac_2]$ (16.1 mg), $H_4[Cu_2(R^{2-})_2(R^-)_4enAc]$ (16.4 mg) and $Na_8[Cu_2(R^{2-})_6]$ (25.2 mg) in mixtures of concentrated nitric acid, per chloric acid and sulfuric acid. Each sample was diluted to 50 mL using distilled water. After the known concentration obtained each solutions were further diluted then the metal contents were recorded.

3.2.2.2.2. Ultra violet-visible spectroscopy

The electronic spectra of the ligands, metal salt and Cu (II) complexes were determined using Sanyo SP65 UV-Vis double beam spectrophotometer in ethanol solution in the range 200-800 nm at room temperature by taking ethanol as a blank. The electronic spectra were able to provide information about the electronic transition that took place within the molecular orbital of the metal, or the ligands that were present in the metal complexes.

3.2.2.2.3. FT-IR spectroscopy of the ligands and the Cu (II) complexes

The infrared spectra of the synthesized copper (II) complexes were obtained using Perkin Elmer FT-IR BX spectrophotometer in the range of 4000 - 400cm^{-1}. Each sample was mixed with dried IR-grade KBr powder and ground until no crystalline material was observed to prevent scattering effect. After that, small amount of sample was subjected to compression with a manual hydraulic press for characterization.

3.2.2.3.Electrochemical characterization

The cyclic voltammetry experiments were carried out in 1 $mmoldm^{-3}$, pH = 7.0 NaH_2PO_4_Na_2HPO_4 buffer solution. These experiments were conducted in a three-component cell consisting of a Platinum wire as auxiliary electrode, a non-aqueous reference electrode (Ag/Ag+), and a glassy carbon as working electrode in the range of 1.5 to -1.5 V, with a scan rate of 100 mVs^{-1}[**33**]. The electrochemical measurements were carried out with a slight modification of a method used in Zeng, et al, 2002.

3.3. In vitro antibacterial activity test

3.3.1. Bacterial strains

The antibacterial activities of the ligands, metal salt and homobinuclear metal complexes were tested against the four bacterial strains two gram negative bacteria (Escherichia coli and Klebsiella pneumonia) and two gram positive bacteria (Staphylococcus aurous and Streptococcus pyogens) by agar disk diffusion method.

3.3.2. Bioassay

The antibacterial test was performed by using agar well disc diffusion method. The bacterial isolates (ATCC) type, were grown in Petri dishes containing Mueller-Hinton agar using a sterile cotton swab. Then 6 mm diameter sterile discs (Whiteman No 3 paper) were placed on the surface of the inoculated agar in Petridishes. And a certain concentrations of the ligands, salt and complexes in appropriate solvent were applied to the discs. The same volume of solvents (water and ethanol) and the standard drug (gentamycin) were used as negative and positive controls respectively for comparison of antibacterial activity. After addition of test solutions on the discs, the solution would allowed to diffuse for 5-10 minutes and the plates were kept in an incubatator at 37 °C until 24 h [**34**]. The antibacterial activities were determined by measuring the zone of inhibition. And the minimum inhibitory concentration (MIC by serial dilution method) of targeted complexes with various concentrations such as 700 ppm, 500 ppm, 300 ppm and 100 ppm were determined. Finally, the antibacterial activity of the ligands and complex were compared with the standard and % activity index for the complex were calculated. The antibacterial tests were carried out in Bahir Dar University, microbiology laboratory, Bahir Dar, Ethiopia.

4. RESULT AND DESCUSSION

4.1. Physicochemical data

4.1.1. Solubility of the complexes

Solubility is one of a characteristic property of a substance. Most of the synthesized complexes were found soluble in polar solvents including methanol, ethanol, acetone and acetonitrile. But, insoluble in nonpolar solvent like dichloromethane which indicates the polar nature of the complexes. $H_4[Cu_2(R^{2-})_2(R^-)_4]$ is partially soluble in water but completely soluble in ethanol and methanol as shown in Table 1. This indicates the complex anion is extremely soft that it poorly interacts with the hard nature of water molecules. The same argument is applied for $H_4[Cu_2(R^{2-})_2(R^-)_4Ac_2]$ and $H_4[Cu_2(R^{2-})_2(R^-)_4enAc]$. Addition of acetone decreases polarity and increasing softness due to the increment of carbon content. So, $H_4[Cu_2(R^{2-})_2(R^-)_4Ac_2]$ and $H_4[Cu_2(R^{2-})_2(R^-)_4enAc]$ were completely insoluble in water still intact but readily soluble in ethanol and methanol.

Table 1: The solubility of the synthesized Cu (II) complexes

Complexes	Solvents								
	water	Methanol	Ethanol	Acetone	Aceto nitrile	EtO Ac	THF	DCM	Diethyl ether
$H_4[Cu_2(R^{2-})_2(R^-)_4]$	P	S	S	S	S	S	S	Ins	P
$H_4[Cu_2(R^{2-})_2(R^-)_4Ac_2]$	Ins	S	S	S	S	S	S	Ins	P
$H_4[Cu_2(R^{2-})_2(R^-)_4enAc]$	Ins	S	S	S	S	S	S	Ins	P
$H_8[Cu_2(R^{2-})_6en_2]$	S	S	S	S	S	S	S	Ins	P
$H_8[Cu_2(R^{2-})_6en]$	S	S	S	S	S	S	S	Ins	P
$Na_8[Cu_2(R^{2-})_6]$	S	S	S	Ins	Ins	Ins	Ins	Ins	Ins

Note:- S- Soluble, P- partial soluble and Ins-Insoluble

4.1.2. Qualitative chloride test

The qualitative chloride test reveals that no white cloudy precipitate was formed indicating the absence of ionizable chlorides outside the coordination sphere.

4.1.3. Color and melting/decomposition temperature determination

Melting point is the temperature at which the solids substances melts or fused. Color is also a characteristic property of transition metal complexes observed due to their interaction with visible portion of the electromagnetic spectrum. As presented in Table 2, the different and sharp melting points of the synthesized complexes indicated that they are pure and very different from the starting materials. $H_4[Cu_2(R^{2-})_2(R^-)_4]$ has higher melting point due to its polar nature and symmetry. Besides, it can probably form H-bonding with the adjacent monoanionic resorcinol. However, the other complexes have relatively lower melting point. This is due to the decreasing of symmetry following the coordination of ethylenediamine and acetone. $Na_8[Cu_2(R^{2-})_6]$ also has relatively low melting point as compared to $H_4[Cu_2(R^{2-})_2(R^-)_4]$. This is probably due to lose of H-bonding upon treated with base.

4.1.4. pH measurement

Most of the synthesized complexes were acidic in nature which strongly agrees with the proposed formula. Thus, R^- and R^{2-} are a σ and π-base ligands which makes the anion of $H_4[Cu_2(R^{2-})_2(R^-)_4]$, very soft nearly complete dissociation is expected. Consequently, after the coordination of acetone and ethylenediamine the extent of dissociation increases. This is evident from the pH value indicated in Table 2. On the other hand, $Na_8[Cu_2(R^{2-})_6]$ is basic according to the pH data.

4.1.5. Molar conductivity measurement

Electrolytic conductivity measurement has frequently been used in mode of coordination within the limits of their solubility and provides a method of testing the degree of ionization of the complexes, the molecular ions that a complex liberates in solution [**35**]. The molar conductivity values show the complexes to be classified as nonelectrolytes. This is due to the higher molar mass or surface area of the complex anions and strong hydration (solvation) of the cations by solvents. Both factors result in the reduction of the speed of mobility of the particles as a result of the decrease in the kinetic energy imparted by the electric field from measurement instrument [**36**].The molar conductivity was calculated by the following formula.

$$\Lambda M = \frac{1000 \times K}{C}$$

Where, ΛM - molar conductance(S cm^2 mol^{-1}), K-specific conductance(Scm^{-1}), C- concentration (Mole/L).

Table 2: The physicochemical results of the synthesized Cu (II) complexes

Complexes	Color	Expected Mwt (g/mole)	Yield (%)	M.pt T^0 (^{0}C)	pH	Molar conductivity (S cm^2 mol^{-1})
$H_4[Cu_2(R^{2-})_2(R^-)_4]$	reddish brown	783.76	88.4	243	4.203	4.32
$H_4[Cu_2(R^{2-})_2(R^-)_4Ac_2]$	Plum	899.76	85.6	113	3.411	6.31
$H_4[Cu_2(R^{2-})_2(R^-)_4enAc]$	Maroon	901.96	86.2	80	3.745	1.62
$H_8[Cu_2(R^{2-})_6en_2]$	saddle brown	903.8	82.7	126	3.745	4.84
$H_8[Cu_2(R^{2-})_6en]$	Pink	843.78	83.0	126	3.782	4.61
$Na_8[Cu_2(R^{2-})_6]$	Wine	871.76	85.5	123	10.02	33.2

4.2. Spectroscopic data

4.2.1. Metal content determination / ICP-OES measurement

The ICP-OES spectrometer measurement (Table-3) results were almost in agreement with the calculated values based on the proposed formula of the complexes.

Table 3: Metal composition of the complexes

Complexes	Cu concentration in ppm		Na concentration in ppm	
	Calculated value	Measured value	Calculated value	Measured value
$H_4[Cu_2(R^{2-})_2(R^-)_4]$	4.849	4.643	-	-
$H_8[Cu_2(R^{2-})_6en_2]$	3.670	3.475	-	-
$H_8[Cu_2(R^{2-})_6en]$	11.120	11.07	-	-
$H_4[Cu_2(R^{2-})_2(R^-)_4Ac_2]$	5.186	5.139	-	-
$H_4[Cu_2(R^{2-})_2(R^-)_4enAc]$	7.857	7.616	-	-
$Na_8[Cu_2(R^{2-})_6]$	11.590	11.410	4.250	3.327

4.2.2. UV-Vis spectra of the ligands and the Cu (II) complexes

The UV-visible spectra of the ligands, metal salt and the synthesized metal complexes were recorded in ethanol in the wavelength range of 200-800 nm. Typically, a shift in Uv-Visible maximum (λ_{max}) of the free ligands is expected after coordinated to a metal ion, forming metal complexes due to the modifications in electronic distribution. Table 4 shows the UV-Vis spectral results of the ligands, metal salt and the synthesized complexes.

The UV-Visible absorption spectrum of resorcinol showed two absorption bands at 274 nm and 326 nm attributed to $\pi \rightarrow \pi^*$ (C=C) transition and $n \rightarrow \pi^*$ transition were shifted to 222 nm and 281 nm in the spectrum of $H_4[Cu_2(R^{2-})_2(R^-)_4]$ Figure 7. Additionally, the band at 331 nm from the spectrum of $CuCl_2.2H_2O$ attributed to MLCT or LMCT shifted to 326 nm in the spectrum of $H_4[Cu_2(R^{2-})_2(R^-)_4]$ complex indicates the formation of complex. Furthermore, the presence of non-ligand band at 484 nm in the expanded spectrum corresponding to d-d transition ($^2T_{2g} \rightarrow {}^2E_g$) confirms the formation of complex.

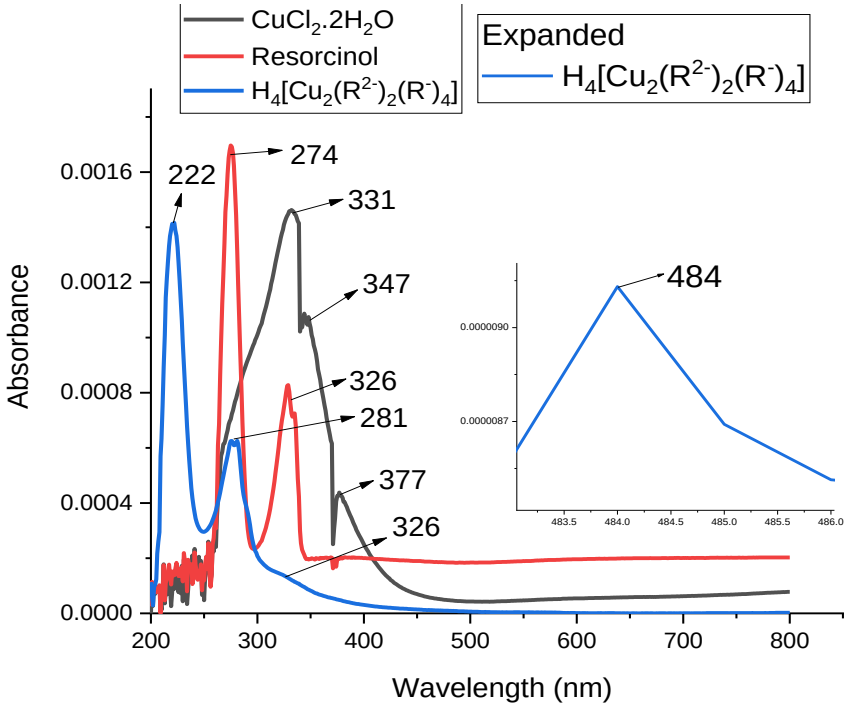

Figure 7: The UV-Vis spectra of the ligands, metal salt and $H_4[Cu_2(R^{2-})_2(R^-)_4]$ with expanded spectra.

The absorption band from the spectrum of $H_4[Cu_2(R^{2-})_2(R^-)_4]$ at 281 nm attributed to $\pi \rightarrow \pi^*$ (C=C) transition is shifted to 279 nm in the spectrum of $H_4[Cu_2(R^{2-})_2(R^-)_4Ac_2]$ due to the

coordination of acetone. Such band comes from resorcinol moiety but shifted to the shorter wave length (blue shift). The blue shift is due to the increasing of the energy gap between π and π* as a consequence of the increasing in electron density on π bonding molecular orbital following coordination of acetone. As shown in Figure 8, the peak from the spectrum of acetone at 321nm attributed to π →π* (C=O) transition shifted to 335 nm upon coordination. And the band 345 nm attributed to n →π* (C=O) transition is also present in the spectrum of $H_4[Cu_2(R^{2-})_2(R^-)_4Ac_2]$ complex verify the coordination of acetone. And the presence of non-ligand bands at 385 nm and 655 nm corresponding to MLCT or LMCT and d-d transition ($^2T_{2g}\rightarrow{}^2E_g$) respectively in the expanded spectrum further justifies the formation of the complex.

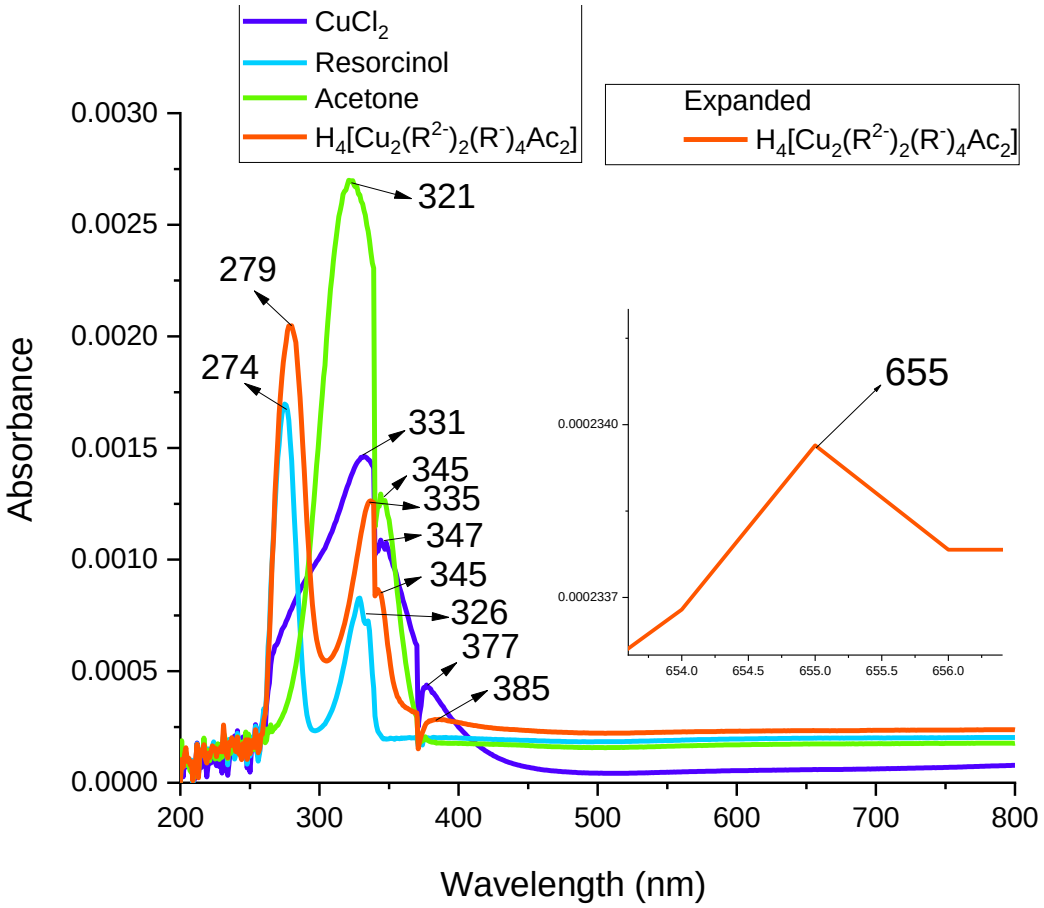

Figure 8: The UV-Vis spectra of the ligands, metal salt and $H_4[Cu_2(R^{2-})_2(R^-)_4Ac_2]$ with expanded spectra.

The band in the $H_4[Cu_2(R^{2-})_2(R^-)_4Ac_2]$ complex assigned to C=C (π→π*) at 279 nm was shifted to longer wavelength by 13 nm to 292 nm upon coordination of ethylenediamine. This red shift is due to the decreasing of the energy gap between π and π* as a consequence of the decreasing

in electron density on π bonding molecular orbital following coordination of ethylenediamine. As indicated in Figure 8 and 9, the bands from the spectrum of $H_4[Cu_2(R^{2-})_2(R^-)_4Ac_2]$ at 335 nm, 345 nm and 385 nm are due to π →π* (C=O), n →π* (C=O) transition and metal to ligand charge transfer respectively. The second band shifted to 350 nm in the spectrum of $H_4[Cu_2(R^{2-})_2(R^-)_4enAc]$. Besides, $H_4[Cu_2(R^{2-})_2(R^-)_4enAc]$ exhibited non-ligand band in the expanded spectrum of visible region at 701 nm attributed to d-d transition($^2T_{2g}\rightarrow{}^2E_g$).

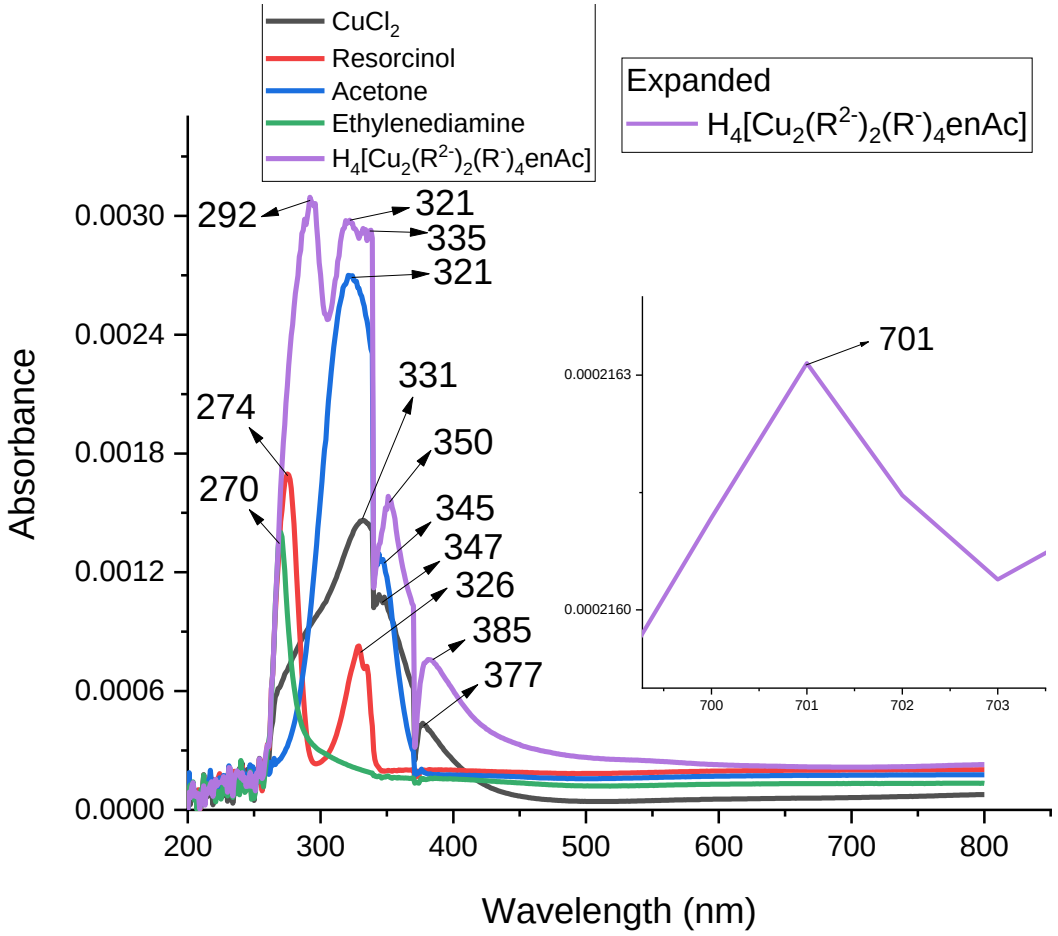

Figure 9: The UV-Vis spectra of the ligands, metal salt and $H_4[Cu_2(R^{2-})_2(R^-)_4enAc]$ with expanded spectra.

The bands from the spectrum of $H_4[Cu_2(R^{2-})_2(R^-)_4]$ at 281nm and 326 nm corresponding to π →π* (C=C) transition and metal to ligand charge transfer are shifted to 274 nm and 330 nm in the spectrum of $H_8[Cu_2(R^{2-})_6en_2]$ respectively indicates the coordination of ethylenediamine as

shown in Figure 10. The red shift is due to the decreasing of the energy gap between π and π* as a consequence of the decreasing in electron density on π bonding molecular orbital. The band at 270 nm from free ethylenediamine attributed to n →σ* (C-N) shifted to 281 nm in $H_8[Cu_2(R^{2-})_6en_2]$ following coordination of ethylenediamine. The presence of non-ligand band from the expanded spectrum of $H_8[Cu_2(R^{2-})_6en_2]$ at 543nm attributed to d-d transition($^2T_{2g}\rightarrow{}^2E_g$).

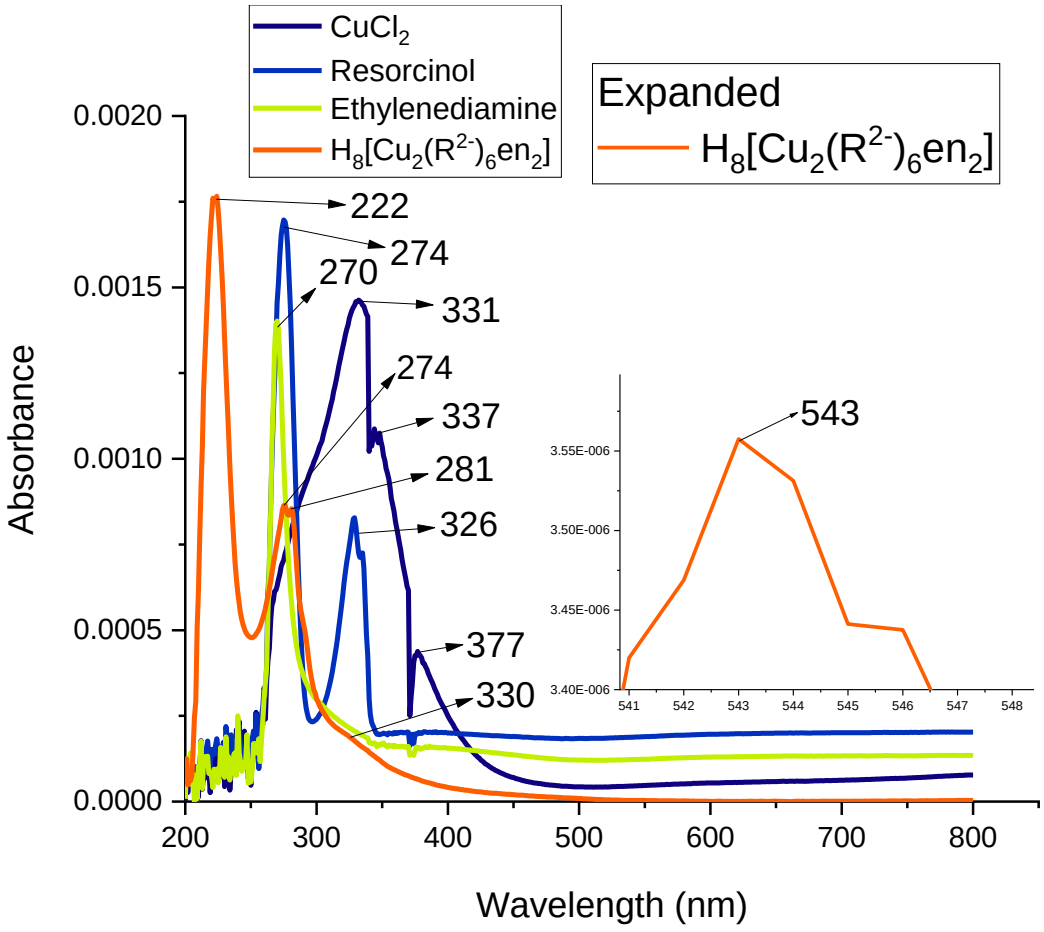

Figure 10: The UV-Vis spectra of the ligands, metal salt and $H_8[Cu_2(R^{2-})_6en_2]$ with expanded spectra.

The bands from the spectrum of $H_4[Cu_2(R^{2-})_2(R^-)_4]$, 222 nm, 281 nm and 326 nm are shifted to 225 nm, 284 nm and 338 nm in the spectrum of $H_8[Cu_2(R^{2-})_6en]$ respectively are attributed to π →π* (C=C) transition, n →π* transition and metal to ligand charge transfer indicates the coordination of ethylenediamine see Figure 11. Additionally, the band from the spectrum of

$H_8[Cu_2(R^{2-})_6en_2]$ at 330 nm is shifted to 338 nm indicates the coordination of ethylenediamine by two ends. The red shift is due to the decreasing of the energy gap between π and π* as a consequence of the decreasing in electron density on π bonding molecular orbital following coordination of ethylenediamine by two ends. The presence of non-ligand band from the expanded spectrum of $H_8[Cu_2(R^{2-})_6en]$ at 479 nm attributed to d-d transition($^2T_{2g} \rightarrow {}^2E_g$) is different from the spectrum $H_8[Cu_2(R^{2-})_6en_2]$.

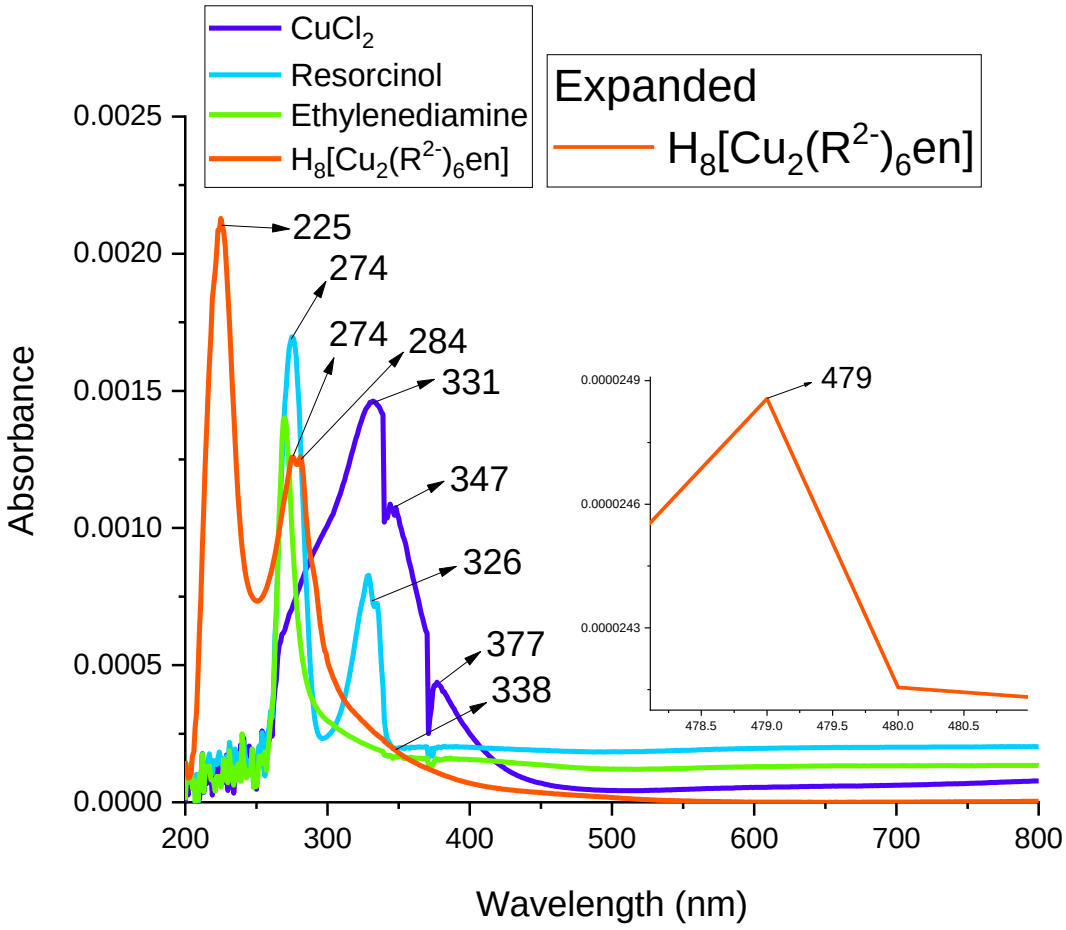

Figure 11: The UV-Vis spectra of the ligands, metal salt and $H_8[Cu_2(R^{2-})_6en]$ with expanded spectra.

The UV-Visible absorption spectrum of free resorcinol showed two absorption bands at 274 nm and 326 nm attributed to π →π* (C=C) transition and n →π* transition were shifted to 230 nm and 276 nm in the spectrum of $Na_8[Cu_2(R^{2-})_6]$. The UV-Visible absorption spectrum of

$CuCl_2.2H_2O$ salt at 331 nm, 347 nm and 377 nm attributed to MLCT were shifted to 326 nm, 340 nm and 385 nm indicates the coordination of resorcinol to the metal center. Figure 12 shows, the presence of intense peak different from the starting materials at 501nm attributed to d-d transition ($^2T_{2g} \rightarrow {}^2E_g$) further confirms the formation of the complex.

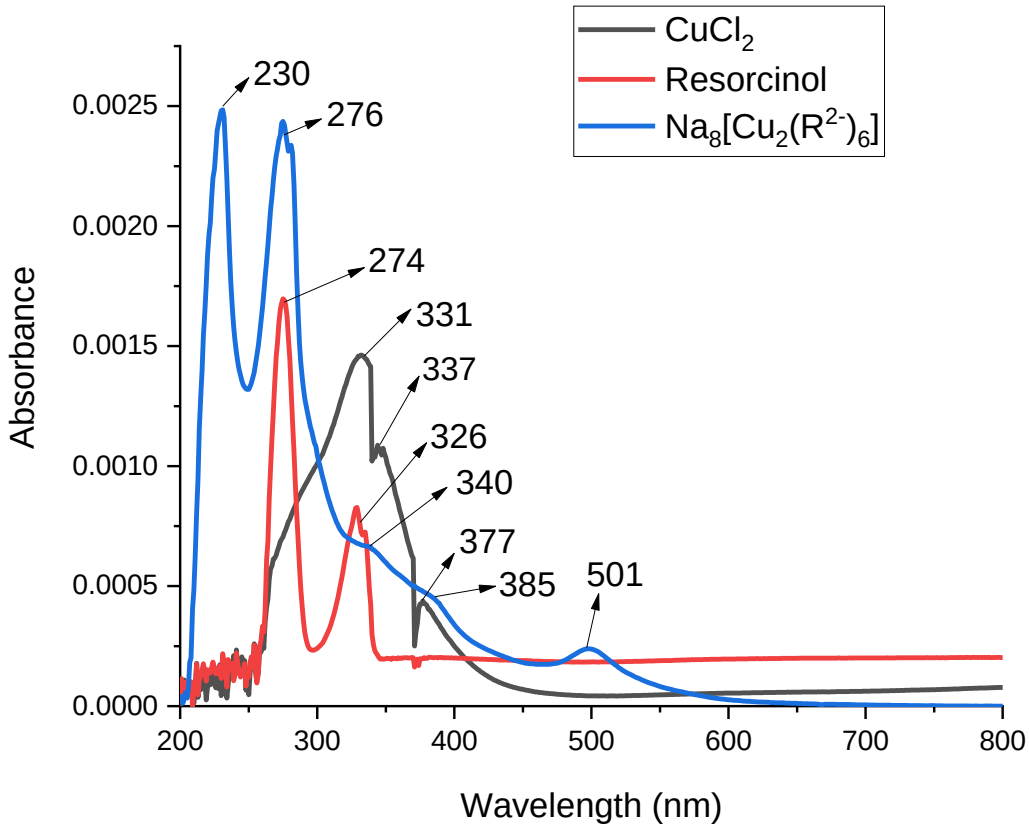

Figure 12: The UV-Vis spectra of the ligands, metal salt and $Na_8[Cu_2(R^{2-})_6]$.

Table 4: The UV-Vis spectral results of the ligands, metal salt and the synthesized complexes in ethanol.

Compounds	Absorption Bands (nm)	Type of transitions
Resorcinol	274, 326	$\pi\rightarrow\pi^*$(C=C), $n\rightarrow\pi^*$
Ethylenediamine	270	$n\rightarrow\sigma^*$ (C-N)
Acetone	321, 345	$\pi\rightarrow\pi^*$(C=C),$n\rightarrow\pi^*$(C=O)
$CuCl_2.2H_2O$	331,347,377	LMCT
$H_4[Cu_2(R^{2-})_2(R^-)_4]$	222,281 326 484	$\pi\rightarrow\pi^*$(C=C) LMCT d-d Transition ($^2T_{2g}\rightarrow{}^2E_g$)
$H_4[Cu_2(R^{2-})_2(R^-)_4Ac_2]$	279,335 345,385 655	$\pi\rightarrow\pi^*$(C=C),$\pi\rightarrow\pi^*$(C=O) $n\rightarrow\pi^*$(C=O), LMCT d-d Transition($^2T_{2g}\rightarrow{}^2E_g$)
$H_4[Cu_2(R^{2-})_2(R^-)_4enAc]$	292,335 350,385 701	$\pi\rightarrow\pi^*$(C=C),$n\rightarrow\pi^*$(C=O) $n\rightarrow\pi^*$(C=O), LMCT d-d Transition($^2T_{2g}\rightarrow{}^2E_g$)
$H_8[Cu_2(R^{2-})_6en_2]$	222,281 330 543	$\pi\rightarrow\pi^*$(C=C) LMCT or MLCT d-d Transition($^2T_{2g}\rightarrow{}^2E_g$)
$H_8[Cu_2(R^{2-})_6en]$	225,284 338 479	$\pi\rightarrow\pi^*$(C=C) LMCT or MLCT d-d Transition($^2T_{2g}\rightarrow{}^2E_g$)
$Na_8[Cu_2(R^{2-})_6]$	230,276 340,385 501	$\pi\rightarrow\pi^*$(C=C) LMCT or MLCT d-d Transition($^2T_{2g}\rightarrow{}^2E_g$)

4.2.3. FT-IR spectra of the ligands and the Cu (II) complexes

The characteristic bands in free resorcinol at 3250 cm^{-1}(s), 3018 cm^{-1} and 1613 cm^{-1}(s) are due to (O-H),(C-H) and (C=C), respectively, are shifted to 3327 cm^{-1}(s), 3002 cm^{-1} and 1604 cm^{-1}(s), in $H_4[Cu_2(R^{2-})_2(R^-)_4]$ complex see Figure 13 and 14. The broadness of the band at 3327 cm^{-1} (s and b) in $H_4[Cu_2(R^{2-})_2(R^-)_4]$ is presumably corresponding to the free O-H stretching of R^- (which may be form hydrogen bonding) or water of crystallization exist due to hygroscopic nature of the complex. The full deprotonation for the two bridging resorcinolate anions was achieved in THF. In addition to negative inductive effect to the ring system, when the free ligand resorcinol approaches to the metal ion *via* coordinate covalent bond formation, the bond between oxygen and hydrogen (O-H) weakens and increases the acidity of resorcinol. At that moment, the lone pair of oxygen atom assisted by two alkyl groups of THF abstracts a proton. This phenomenon is due to the acidic nature of resorcinol bind with a metal ion.

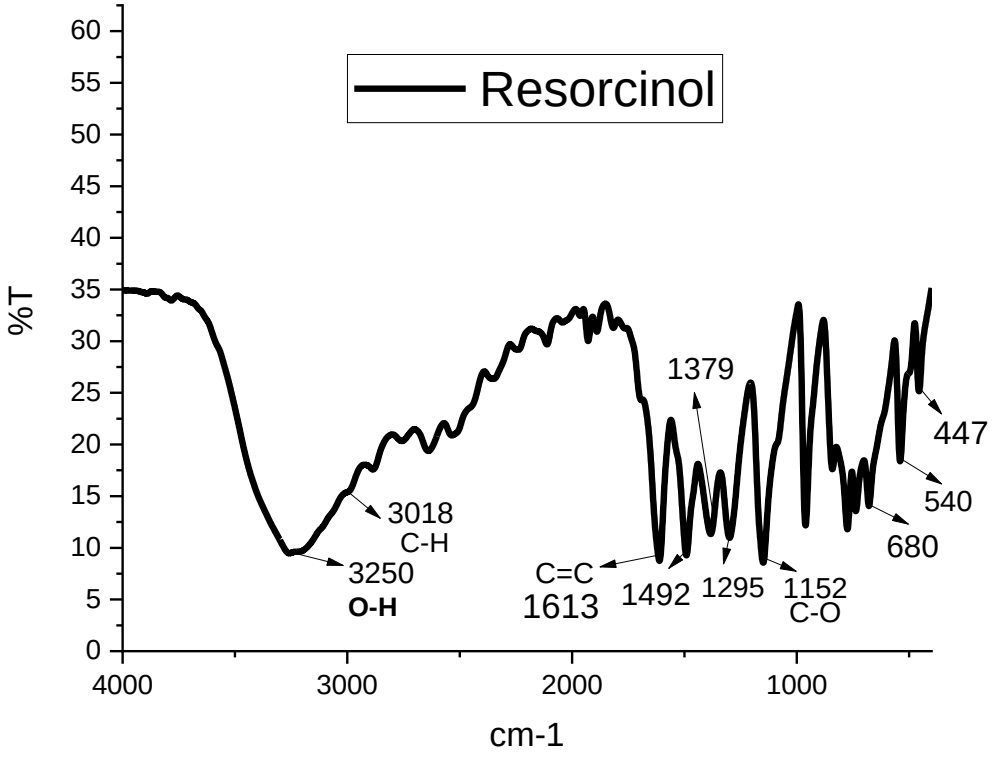

Figure 13: The IR spectrum of Resorcinol

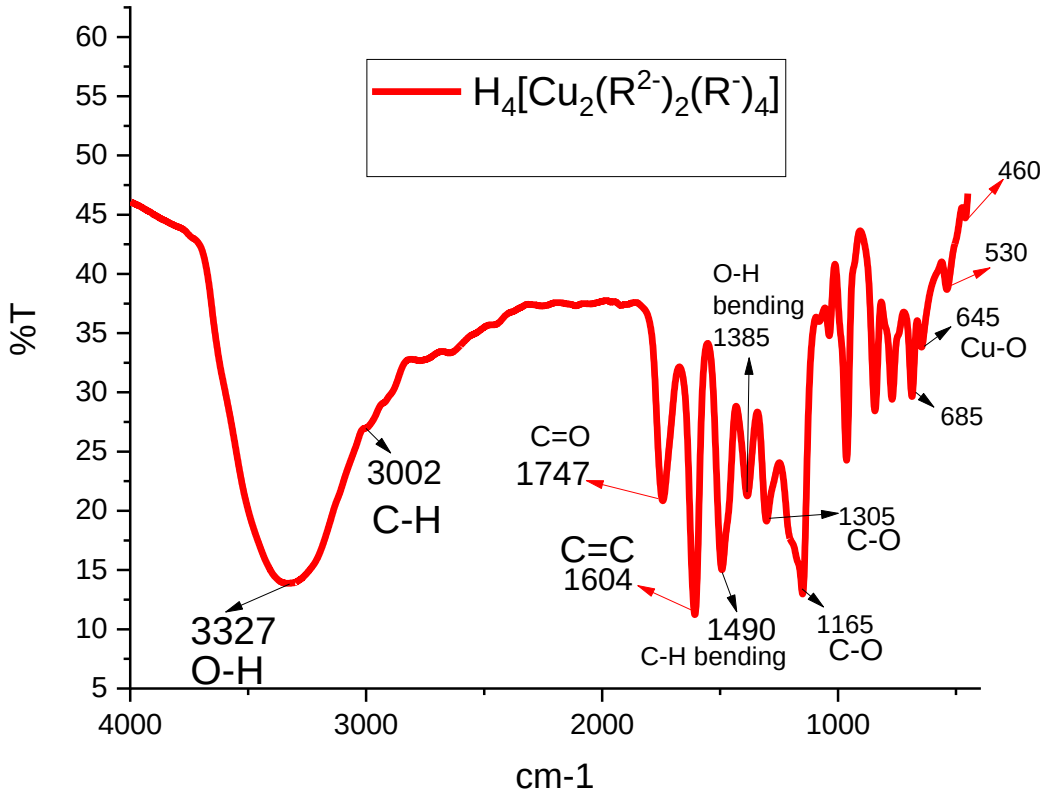

Figure 14: The IR spectrum of $H_4[Cu_2(R^{2-})_2(R^-)_4]$.

Besides, the presence of new peak around 1747cm^{-1} (m) which is absent from IR spectrum of resorcinol (ligand) may be corresponding to the double bond redistribution around the ring and oxygen atom forms a C=O (phenolate ion) intermediate due to the presence ofπ^* molecular orbital of the ligand resorcinolate leads toπ back bonding forms (C=O) double bond. And also the characteristic bands in free resorcinol at 1152 cm^{-1}(s), 1295cm^{-1}(m) and 1379 cm^{-1}(w) corresponding to C-O, are shifted to1165 cm^{-1}(s), 1305cm^{-1}(m) and 1385cm^{-1}(w) respectively [**37,38**]. Such phenomenon indicates the coordination of resorcinolate with Cu (II) metal. Identification of peaks for υ (M-O) is difficult because these bands can be observed at any value between (400-800) cm^{-1}. But, the new band found in the spectrum of the complex $H_4[Cu_2(R^{2-})_2(R^-)_4]$ lie 645cm^{-1} is not present in the spectrum of resorcinol attributed to ν(M-O).

The coordination of acetone to $H_4[Cu_2(R^{2-})_2(R^-)_4]$ to get $H_4[Cu_2(R^{2-})_2(R^-)_4Ac_2]$ was confirmed by the appearance of new bands at 2961 cm^{-1}(s) and 1680 cm^{-1}(m) are corresponding to sp^3(C-H stretching) and (C=O) respectively as shown in Figure 15. Bond formation between the oxygen of the acetone molecule and the metal ion weakens the C=O bond to some extent, causing a smaller force constant and a lowering of the stretching frequency. The C=O vibration of free acetone at 1718 cm^{-1} shifted to 1677 cm^{-1} up on complexation [**27**]. In this case it appears at1680 cm^{-1}.

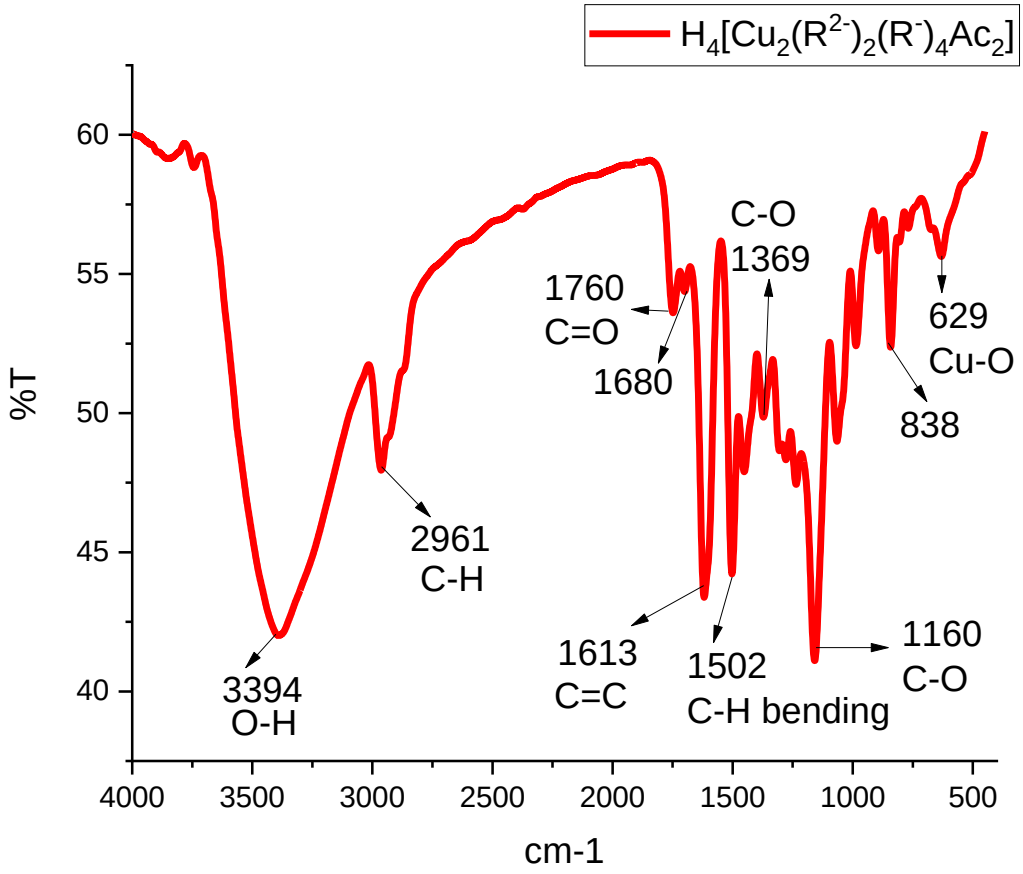

Figure 15: The IR spectrum of $H_4[Cu_2(R^{2-})_2(R^-)_4Ac_2]$.

The characteristic bands in $H_4[Cu_2(R^{2-})_2(R^-)_4]$ complex at 3327 cm^{-1}(s&b), 1747 cm^{-1}(m), 1604 cm^{-1}(s), 1490 cm^{-1}(s), 1165 cm^{-1}(s) and 645 cm^{-1}(w) are due to (O-H), (C=O), (C=C), (C-H bending), (C-O) stretching and (M-O) respectively, are shifted to 3394 cm^{-1}(s&b), 1760 cm^{-1}(w), 1613 cm^{-1}(s), 1502 cm^{-1}(s), 1160 cm^{-1}(s) and 629 cm^{-1}(w) in $H_4[Cu_2(R^{2-})_2(R^-)_4Ac_2]$

complex. The weakness of the band at 1680 cm^{-1}(w) for $H_4[Cu_2(R^{2-})_2(R^-)_4Ac_2]$ is due to the symmetrical nature of the complex leads to decrease change in dipole moment. Bonding between the metal ions and the acetone molecules takes place, presumably, *via* one of the oxygen lone pairs, which means that the C-O-M angle will be about 120" [**27**].

The FTIR spectrum of free ethylenediamine was used for comparison as shown in Figure16.

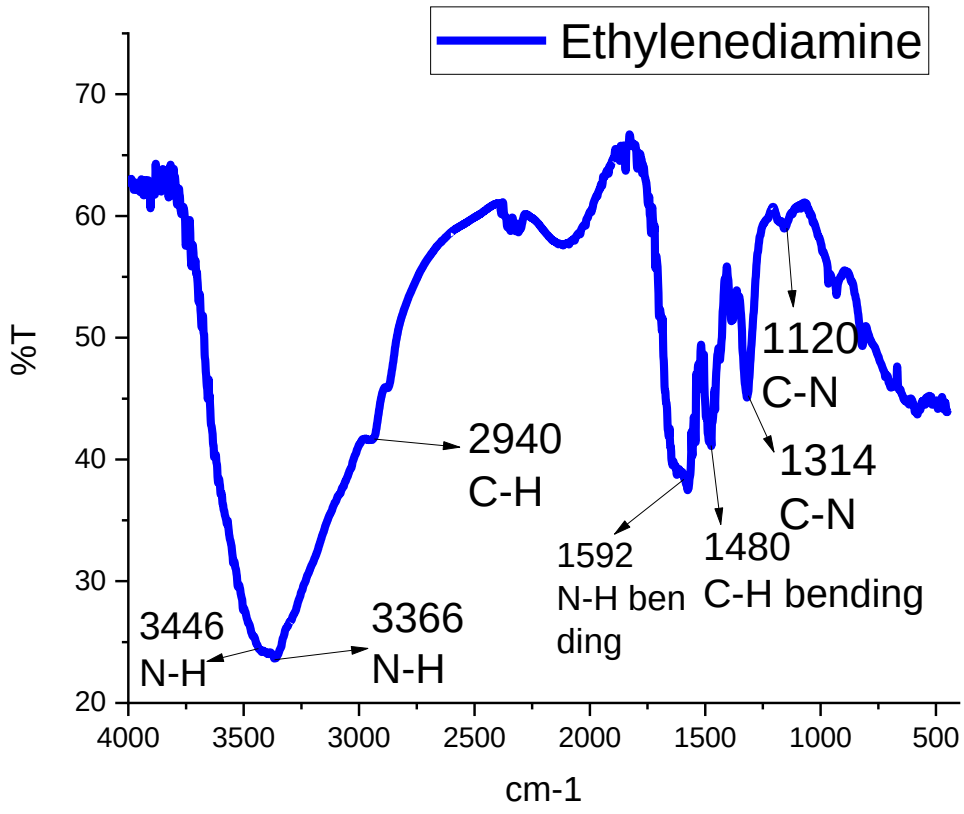

Figure 16: The IR spectrum of Ethylenediamine.

The coordination of ethylenediamine to $H_4[Cu_2(R^{2-})_2(R^-)_4Ac_2]$ to get $H_4[Cu_2(R^{2-})_2(R^-)_4enAc]$ was confirmed by the appearance of new bands at 1040 cm^{-1}(m) and strength of 1680 cm^{-1}(s) for $H_4[Cu_2(R^{2-})_2(R^-)_4enAc]$ are corresponding to (C-N) and (C=O) respectively indicates coordination of ethylenediamine. Figure 17 shows, the peak 1680 cm^{-1}(w) weak for $H_4[Cu_2(R^{2-})_2(R^-)_4Ac_2]$ resolves after the coordination of ethylenediamine by substitute one acetone molecule. The characteristic bands in $H_4[Cu_2(R^{2-})_2(R^-)_4]$ complex at 3327 cm^{-1}(s & b),1747cm^-

^{1}(m), 1604 cm^{-1}(s), 1490 cm^{-1}(s), 1165cm^{-1}(s) and 645 cm^{-1}(w) are due to (O-H), (C=O), (C=C), (C-H bending), (C-O) stretching and (M-O) respectively, are shifted to 3394 cm^{-1}(s & b), 1760 cm^{-1}(w), 1613 cm^{-1}(s), 1502 cm^{-1}(s), 1160 cm^{-1}(s) and 615 cm^{-1}(w) in $H_4[Cu_2(R^{2-})_2(R^{-})_4enAc]$ complex. As well as a new band from the spectra of $H_4[Cu_2(R^{2-})_2(R^{-})_4enAc]$ appears at 489 cm^{-1}(w) is corresponding to (M-N). Very weak bands at 3271 cm^{-1}(w) and 3189 cm^{-1}(w) are attributed to primary amine (N-H) stretching indicates the coordination of ethylenediamine to $H_4[Cu_2(R^{2-})_2(R^{-})_4Ac_2]$. The weakness of such bands is due to overlapping (obscure) with broad peak corresponding to (O-H) stretching.

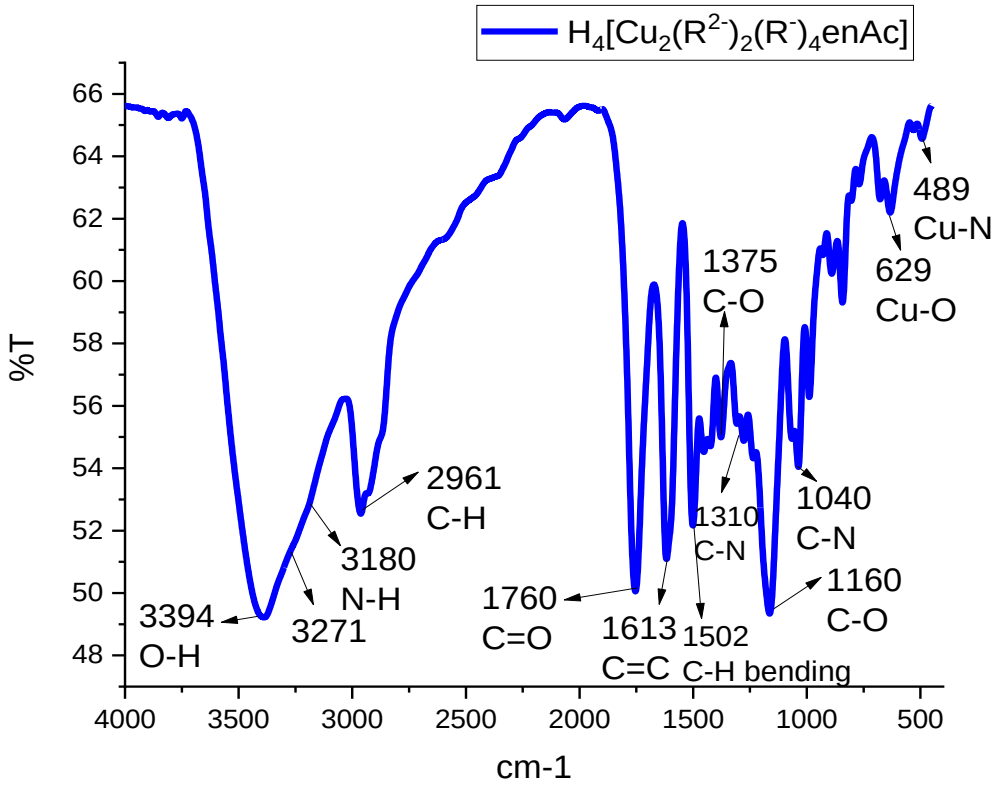

Figure 17: The IR spectrum of $H_4[Cu_2(R^{2-})_2(R^{-})_4enAc]$.

The formation of $H_8[Cu_2(R^{2-})_6en_2]$ from $H_4[Cu_2(R^{2-})_2(R^{-})_4]$ is confirmed by the presence of new bands at 3436 cm^{-1}(s), 3341 cm^{-1}(s) corresponding to primary amine (N-H) stretching and 1028 cm^{-1}(m) attributed to (C-N)stretching Figure 18. The characteristic bands in $H_4[Cu_2(R^{2-})_2(R^{-})_4]$at 1604 cm^{-1}(s) due to (C=C)stretching, 1490 cm^{-1}(s) (C-H) bending and 1385 cm^{-1}(w), 1305 cm^{-1}(m) and 1165 cm^{-1}(s) attributed to (C-O)stretching are shifted to 1604 cm^{-1}(m),1534 cm^{-1} (m),

1360 cm^{-1} (m), 1246 cm^{-1} (w) and 1159 cm^{-1} (w) respectively in the spectrum of $H_8[Cu_2(R^{2-})_6en_2]$ indicates the coordination of ethylenediamine. Identification of peaks for υ (M-O) is difficult because these bands can be observed at any value between 400 cm^{-1} & 800 cm^{-1}. But, the band in the spectrum of the complex $H_4[Cu_2(R^{2-})_2(R^{-})_4]$ lie 645 cm^{-1}(m) is shifted to 600 cm^{-1}(m) attributed to ν(M-O) and new band present in the spectrum of $H_8[Cu_2(R^{2-})_6en_2]$ at 504 cm^{-1}(m) but, absent in the spectrum of $H_4[Cu_2(R^{2-})_2(R^{-})_4]$ attributed to ν(M-N).

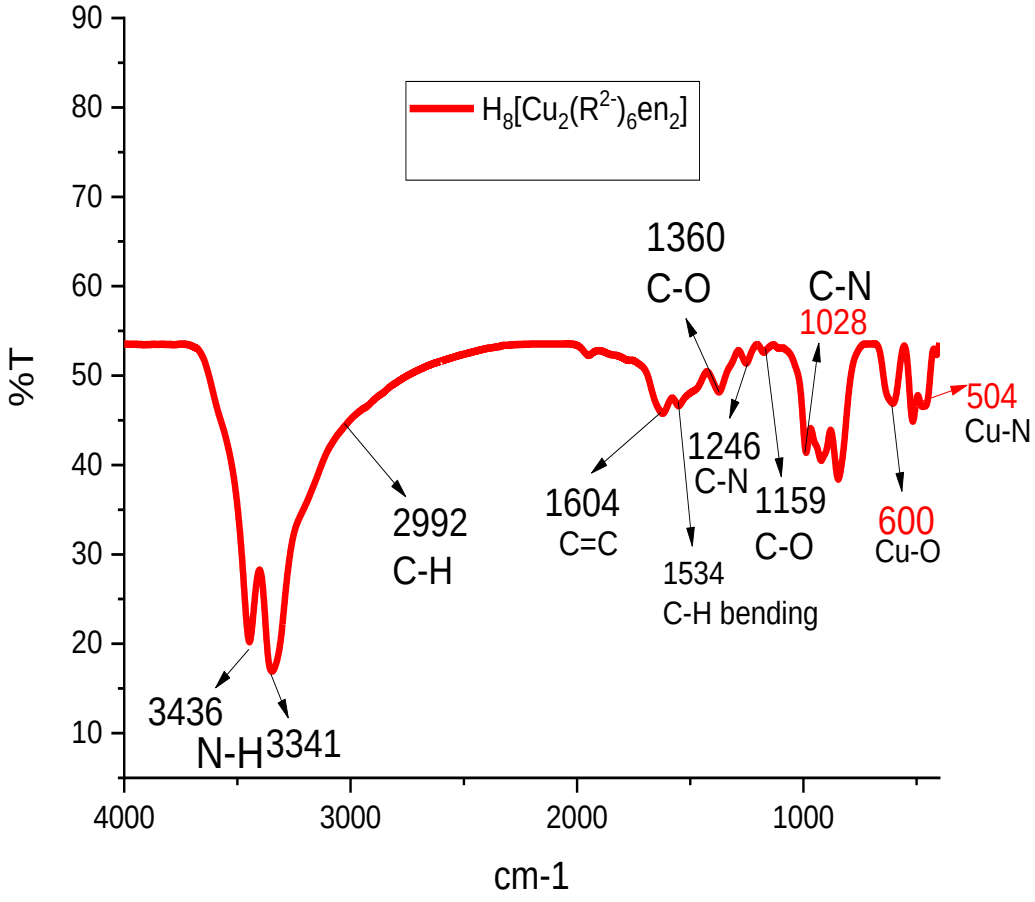

Figure 18: The IR spectrum of $H_8[Cu_2(R^{2-})_6en_2]$.

The formation of $H_8[Cu_2(R^{2-})_6en]$ from $H_4[Cu_2(R^{2-})_2(R^{-})_4]$ is confirmed by the presence of new bands at 3140 cm^{-1}(s), 3045 cm^{-1}(s) corresponding to primary amine (N-H) stretching and 1020 cm^{-1}(m) attributed to (C-N)stretching Figure 19. The characteristic bands in $H_4[Cu_2(R^{2-})_2(R^{-})_4]$ at 3002 cm^{-1}(m) due to (C-H)stretching,1604 cm^{-1}(s) due to (C=C)stretching, 1490 cm^{-1}(s) (C-H)

bending and 1385 cm^{-1}(w), 1305 cm^{-1}(m) and 1165 cm^{-1}(s) attributed to (C-O)stretching are sifted to 2992 cm^{-1}(m), 1592 cm^{-1} (s),1508 cm^{-1} (s), 1360 cm^{-1} (w), 1310 cm^{-1} (w) and 1141 cm^{-1} (w) in the spectrum of $H_8[Cu_2(R^{2-})_6en]$ indicates the coordination of ethylenediamine. Identification of peaks for υ (M-O) is difficult because these bands can be observed at any value between 400 cm^{-1} & 800 cm^{-1}. But, the band in the spectrum of the complex $H_4[Cu_2(R^{2-})_2(R^{-})_4]$ lie 645 cm^{-1}(m) is shifted to 580 cm^{-1}(m) attributed to ν(M-O) and new band present in the spectrum of $H_8[Cu_2(R^{2-})_6en]$at 504 cm^{-1}(w) but, absent in the spectrum of $H_4[Cu_2(R^{2-})_2(R^{-})_4]$ attributed to ν(M-N).

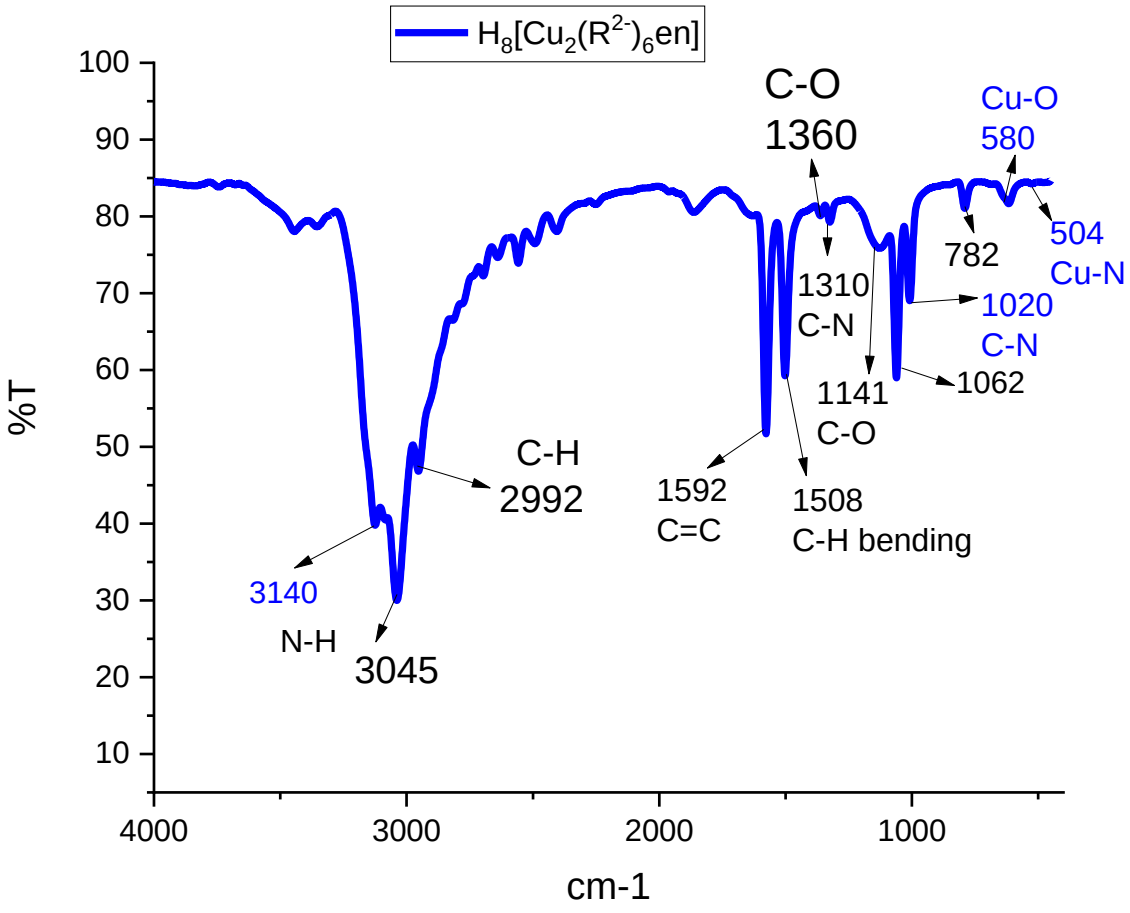

Figure 19: The IR spectrum of $H_8[Cu_2(R^{2-})_6en]$.

The characteristic bands in free resorcinol at 3250 cm^{-1}(s), 1613 cm^{-1}(s) and 1492 cm^{-1} due to (O-H), (C=C) and (C-H bending) respectively, are shifted to 3424 cm^{-1}(s), 1579 cm^{-1}(m & twisted), and 1467 cm^{-1} in the spectrum of $Na_8[Cu_2(R^{2-})_6]$ complex as shown in Figure 20. And also the characteristic bands in free resorcinol at 1152 cm^{-1}(s), 1295 cm^{-1}(m) and 1379 cm^{-1}(w) corresponding to C-O, are shifted to1143 cm^{-1}(s), 1244 cm^{-1} and 1304 cm^{-1}. Additionally, new band found in the spectrum of the complex $Na_8[Cu_2(R^{2-})_6]$ lie 647 cm^{-1} is not present in the spectrum of resorcinol belongs to ν(M-O). The broadness of the band at 3424 cm^{-1} (s and b) in $Na_8[Cu_2(R^{2-})_6]$ is presumably due to water of crystallization exist due to hygroscopic nature of the complex and water of KBr.

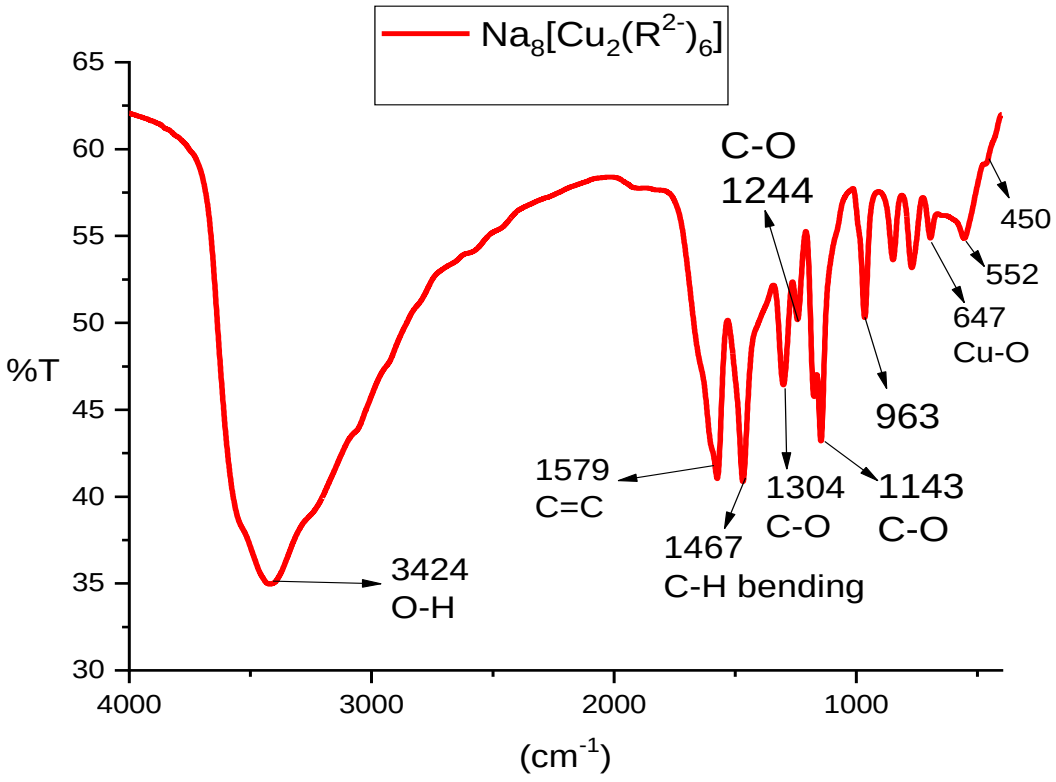

Figure 20: The IR spectrum of $Na_8[Cu_2(R^{2-})_6]$.

The characteristic IR frequencies of resorcinol and the synthesized complexes are listed in table 5 below.

Table 5: The characteristic IR frequencies of ethylenediamine, resorcinol and the complexes.

Compound	Absorption frequencies (cm^{-1})								
	$\nu_{(O-H)}$	$\nu_{(C-H)}$	$\nu_{(C=C)}$	$\nu_{(C-O)}$	**v(C=O)**	**v(N-H)**	**v(C-N)**	**v(Cu-O)**	$\nu_{(Cu-N)}$
Ethylenediamine	-	2940 1580 (s)	-	-	-	3446 (s) , 3366(s)	1120 (w),1414(s)	-	-
Resorcinol	3250 (s & b)	3018 (w)	1613(s)	1152(s) 1295(m) 1379(w)	-	-	-	-	-
$H_4[Cu_2(R^{2-})_2(R^-)_4]$	3327 (s & b)	3002 (w),1490(s)	1604(s)	1165 (s) 1305(m) 1385(w)	1747(m)	-	-	645 (w)	-
$H_4[Cu_2(R^{2-})_2(R^-)_4Ac_2]$	3394 (s & b)	2961 (s)	1613(s)	1160(s)	1760(s), 1680(w)	-	-	629(w)	-
$H_4[Cu_2(R^{2-})_2(R^-)_4enAc]$	3394 (s & b)	2961 (s)	1613(s)	1160(s)	1760(s)	3271(w) & 3180(w)	1417 (w),1040(m)	629(w)	489 (w)
$H_8[Cu_2(R^{2-})_6en_2]$	-	2992 (w)	1604 (w)	1159 (m)	-	3436(s), 3341(s)	1028(m)	600(w)	504(w)
$H_8[Cu_2(R^{2-})_6en]$	-	2992 (m)	1592(s)	1141(w)	-	3140(s)	1020 (m)	580(w)	504 (w)
$Na_8[Cu_2(R^{2-})_6]$	3424 (s & b)	1467 (s)	1579(s) twisted	1143(s)	-	-	-	647(w)	-

4.3. Electrochemical characterization

The electrochemical behaviour of the ligand and copper (II) complexes were studied by cyclic voltammetry (CV) in phosphate buffer solution in scanning window between +1.5 and -1.5 V vs Ag/AgCl at scan rate of 0.1 Vs^{-1}. In order to classify these redox peaks as ligand-based or metal-based, the CV of the ligand and the metal salt in water was carried out under the same condition and compared with Cu (II) complexes (Figure 21).

The free ligand resorcinol shows irreversible redox peak at +0.74 V vs Ag/AgCl. However, the potential of irreversible oxidation peak for most of synthesized complexes has shifted to less positive potential as compared to the free ligand resorcinol indicates the formation of complexes. The complexes show ligand-based electrochemical processes because they are resorcinol based complexes. In this regard, the peak at +0.74 V vs Ag/AgCl of free resorcinol was shifted to +0.65 V, +0.69 V, +0.67 V and +0.70 V vs Ag/AgCl for $H_4[Cu_2(R^{2-})_2(R^-)_4]$, $H_8[Cu_2(R^{2-})_6en_2]$, $H_8[Cu_2(R^{2-})_6en]$ and $Na_8[Cu_2(R^{2-})_6]$ respectively verifies the formation of synthesized complexes. Besides, all shifts are to the less positive potential indicates the synthesized complexes have high redox stability. However, the two complexes such as $H_4[Cu_2(R^{2-})_2(R^-)_4Ac_2]$ and $H_4[Cu_2(R^{2-})_2(R^-)_4enAc]$ has no remarkable value due to their water solubility problem.

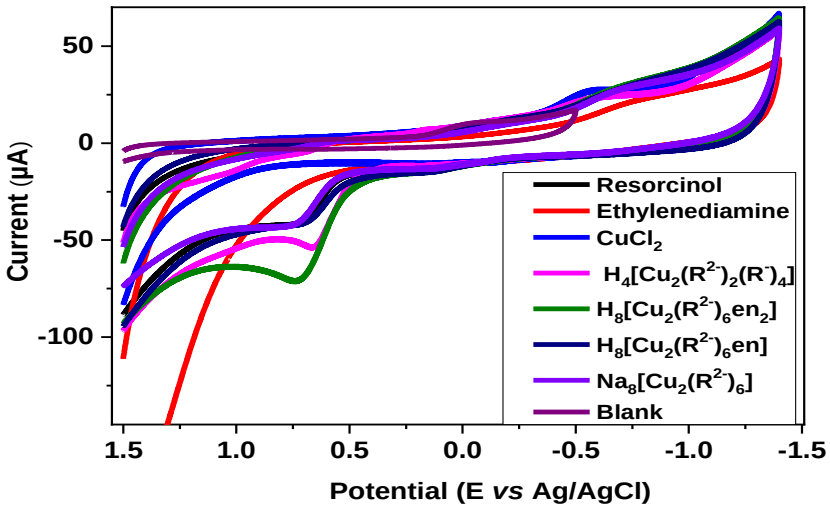

Figure 21:Cyclicvoltamogram of $H_4[Cu_2(R^{2-})_2(R^-)_4]$, $H_8[Cu_2(R^{2-})_6en_2]$, $H_8[Cu_2(R^{2-})_6en]$ and $Na_8[Cu_2(R^{2-})_6]$ with ligands and reference.

4.4. *In vitro* antibacterial activity data

The involvement of metal complexes in medical treatment is of special interest as it is known that bacteria can achieve resistance to antibiotics through biochemical and morphological modifications **[39**].In vitro antibacterial activity of the ligands, metal salt, synthesized complexes and commercially available drugs (gentamycin) were studied against two gram negative (E.Coil & K.pneumonia) and two gram positive (S.aureus & S. Pyogenes) bacteria described in (Table 6).

Table 6: The antibacterial activity of complexes, free ligands, metal salt, solvents and commercial antibiotic.

Compounds	***Antibacterial activity(mean zone diameter(mm) ± SD)***			
	Gram positive bacteria		***Gram negative bacteria***	
	S. aurrus IZ(mm)	***S. pyogenes IZ(mm)***	***E. coli IZ(mm)***	***K. pneumonia IZ(mm)***
Resorcinol	11±0.0	12.8± 0.03	8.7± 0.06	9.7±0.06
Ethylenediamine	15.1 ±0.06	17.1±0.06	16±0.0	12.8±0.03
Acetone	11.6 ±0.06	12±0.0	8±0.0	0±0.0
$CuCl_2.2H_2O$	21±0.05	17±0.0	19.3±0.03	15.8±0.03
$H_4[Cu_2(R^{2-})_2(R^-)_4]$	**46±0.05**	**49±0.5**	**43±0.0**	**41.8±0.03**
$H_8[Cu_2(R^{2-})_6en_2]$	**48.6±0.06**	**47.6±0.06**	**45±0.0**	**46±0.0**
$H_8[Cu_2(R^{2-})_6en]$	**42.6±0.06**	**45.3±0.03**	**41±0.0**	**42.3±0.03**
$Na_8[Cu_2(R^{2-})_6]$	**36±0.0**	34±0.0	**35± 0.0**	**38.3±0.03**
$H_4[Cu_2(R^{2-})_2(R^-)_4Ac_2]$	31±0.0	28±0.0	28±0.0	**39±0.0**
$H_4[Cu_2(R^{2-})_2(R^-)_4enAc]$	16.3±0.03	21.6±0.06	23±0.0	20.3±0.03
Gentamycin	28±0.0	38±0.05	28±0.0	26±0.0
Water	0±0.0	0±0.0	0±0.0	0±0.0
Ethanol	0±0.0	0±0.0	0±0.0	0±0.0

The salt ($CuCl_2.2H_2O$) and the free ligands such as resorcinol, ethylenediamine and acetone have no remarkable antibacterial activity as compared to the standard antibiotic (gentamycin). But, most newly synthesized Cu (II) complexes have higher activity than gentamycin for all tested

bacterial strains except $H_4[Cu_2(R^{2-})_2(R^-)_4enAc]$ and $H_4[Cu_2(R^{2-})_2(R^-)_4Ac_2]$ (for S.pyogenes) as shown Figure in 22, 23 and 24. This indicates the activity of the metal ion against bacteria significantly increases upon coordination. The increased activity of the complexes can be explained on the basis of Overtone's concept and Tweedy's Chelation theory [**40,41**].The biological activity of the metal complex is affected by several factors, including the chelating effect of the ligands, the nature of the donor atom, counter ion that neutralize the complex ion and the geometric structure of the complex. According to Overtone's concept of cell permeability, the lipid membrane that surrounds the cell favors the passage of only the lipid soluble materials due to which liposolubility is an important factor, which controls the activity. Chelation considerably reduces the polarity of the metal ion to a greater extent due to the overlap of the ligand orbital and partial sharing of the positive charge of the metal ion with donor groups. Further, it increases the delocalization of π-electrons over the whole chelate ring and enhances the lipophilicity of the complexes. This increased lipophilicity enhances the penetration of the complexes into lipid membrane of bacteria then disturbs the respiration process of the cell and blocks protein synthesis. Such phenomena, restricts further multiplicity of the microorganisms [**16, 42**].

Furthermore, the mode of action of the compounds may involve formation of a hydrogen bond through the R^- group with the active centers of cell constituents, resulting in interference with the normal cell processes [**8**]. The variation in the effectiveness of different compounds against different organisms depends either on the impermeability of the cells of the microbes or on differences in ribosome of microbial cells [**40**]. Antimicrobial agents interfere with specific processes that are essential for growth and division. Particularly, transition metal complexes induce microbial cell death is centered on the essential microbial cell function that is inhibited by the primary drug-target interaction through intercalation or ligand substitution with the DNA base pairs. Antimicrobial agents can be classified based on the cellular component or system they affect, in addition to whether they kill bacteria (bactericidal agents) or inhibit cell growth but does not kill them (bacteriostatic agents) they act by targeting specific sites of microbes. Well known mechanisms of action of antimicrobial agents include;

- ✓ Interference with cell wall synthesis,
- ✓ Inhibition of protein synthesis,
- ✓ Interference with nucleic acid synthesis,

- ✓ Inhibition of intermediary metabolic pathways and
- ✓ Disruption of the cytoplasm membrane [**43**].

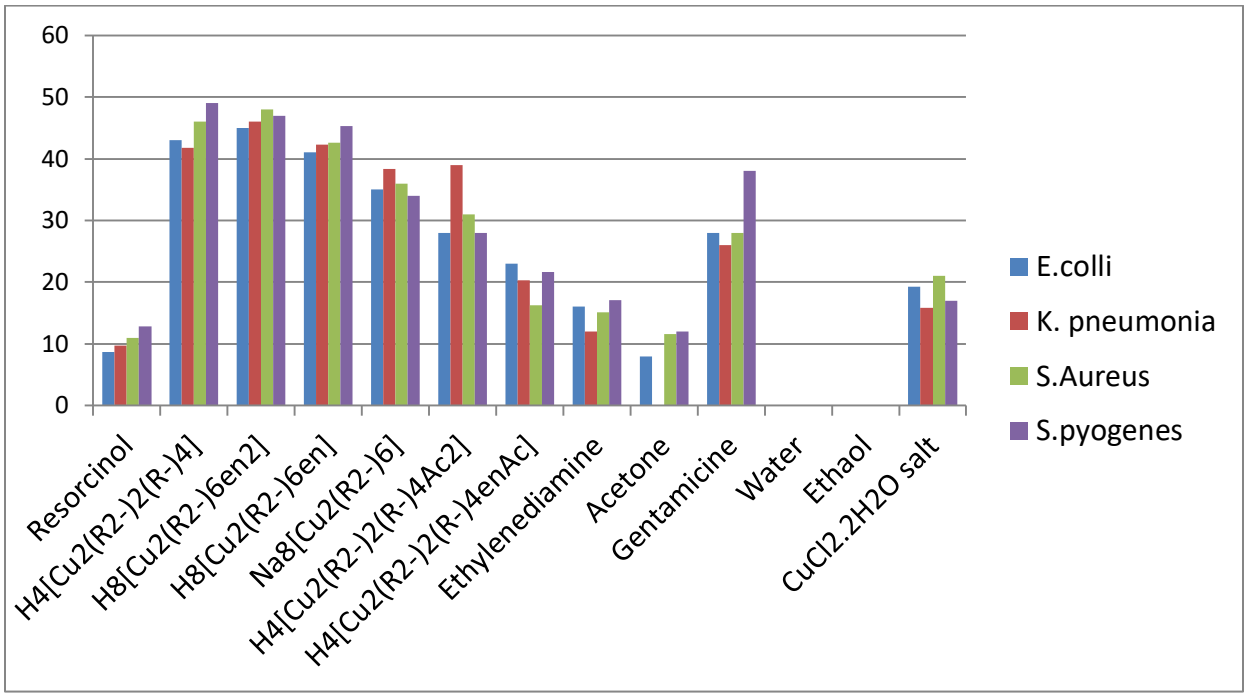

Figure 22: Bar graph for the comparison of antibacterial activity of metal salt, ligands, synthesized complexes, and reference antibiotic drug (gentamycin).

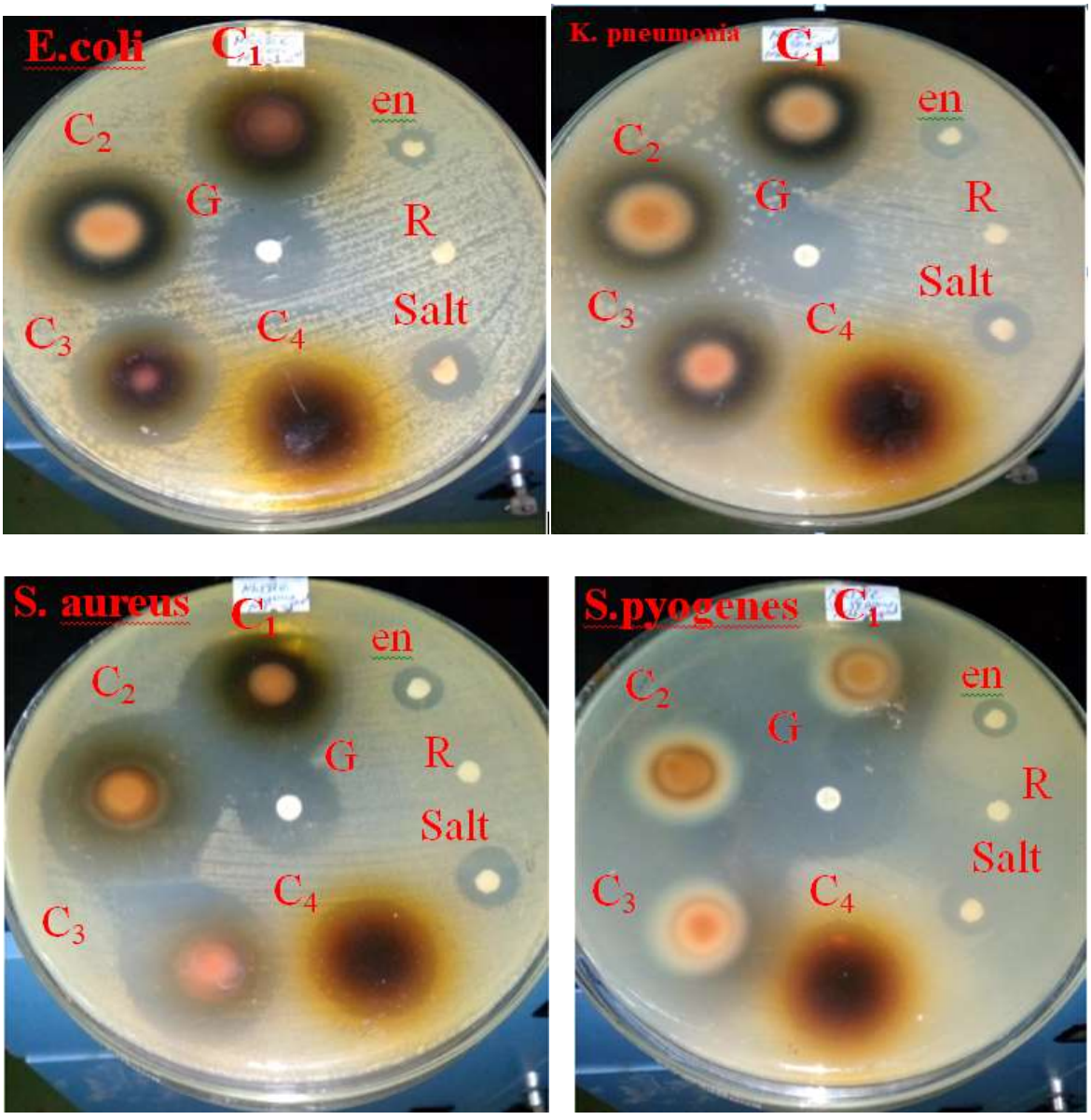

Note:

C_1 = $H_4[Cu_2(R^{2-})_2(R^-)_4]$ R = Resorcinol

C_2 = $H_8[Cu_2(R^{2-})_6en_2]$ Salt = $CuCl_2.2H_2O$

C_3 = $H_8[Cu_2(R^{2-})_6en]$ G = Gentamycin

C_4 = $Na_8[Cu_2(R^{2-})_6]$ en = Ethylenediamine

Figure 23: Inhibition zone of ligands, synthesized complexes, salt, and commercial antibiotic against two Gram-positive and two Gram-negative bacteria.

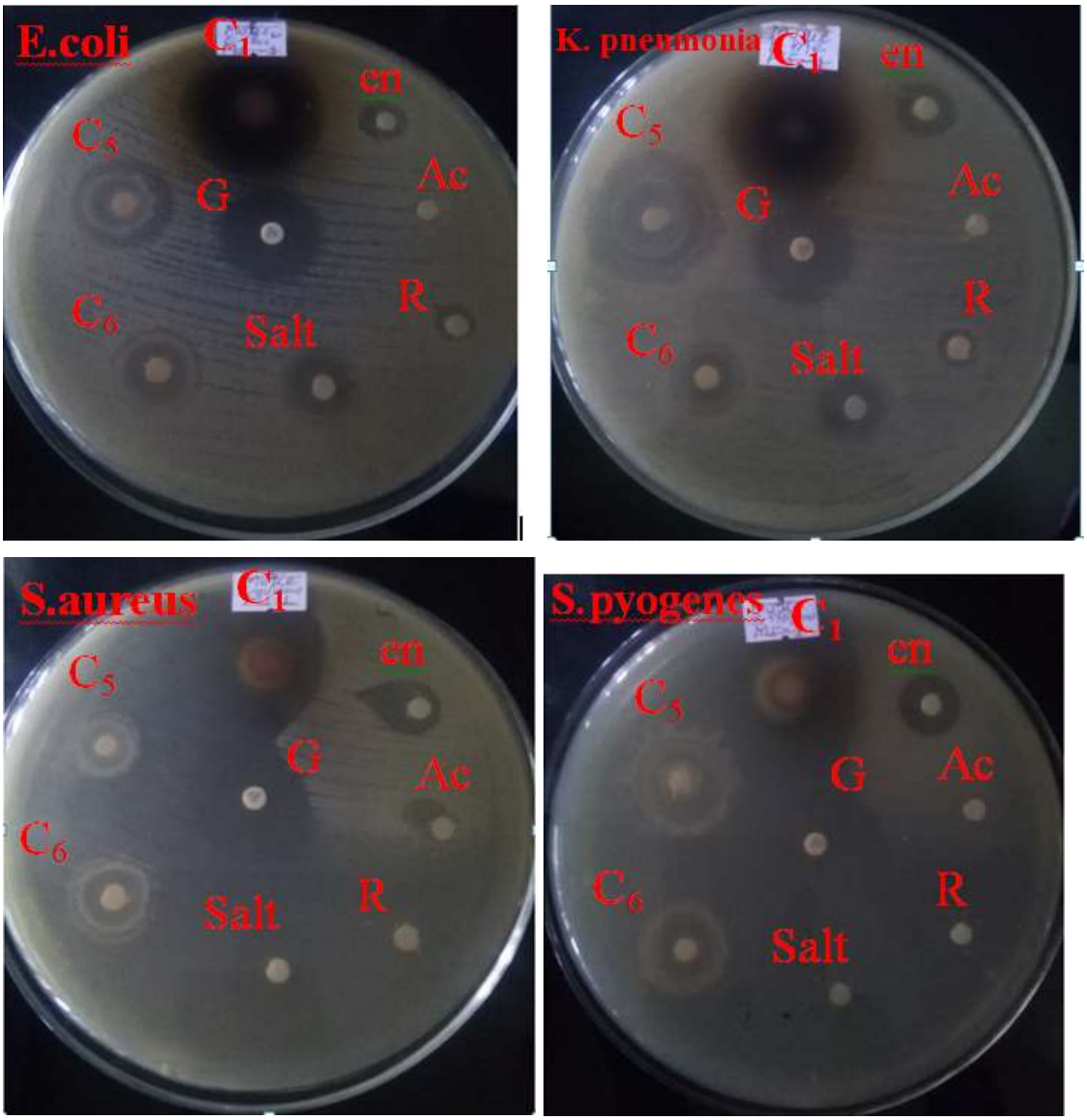

Note:

C_1 = $H_4[Cu_2(R^{2-})_2(R^-)_4]$	R = Resorcinol
C_5 = $H_4[Cu_2(R^{2-})_2(R^-)_4Ac_2]$	G = Gentamycin
C_6 = $H_4[Cu_2(R^{2-})_2(R^-)_4enAc]$	en = Ethylenediamine
Salt = $CuCl_2.2H_2O$	Ac = Acetone

Figure 24: Inhibition zone of ligands, synthesized complexes, salt, and commercial antibiotic against two Gram-positive and two Gram-negative bacteria.

The comparative analysis for the inhibition of the complexes with the reference gentamycin was indicated by the percent activity indexes. % activity index for the complexes were calculated by using the following formula:

$$\%\ \text{Activity index} = \frac{A - B}{B} \times 100$$

Where: A – Zone of inhibition (diameter) of test compound

B – Zone of inhibition (diameter) of reference (gentamycin)

The result demonstrated that most complexes were very active against bacteria and has greater activity than gentamycin See Table- 7.

Table 7: %Activity index data of the complexes against the tested bacteria as compared to Gentamycin

Compounds	**Bacterial strains**			
	S. aurous ***A. index (%)***	***S. pyogenes*** ***A. index (%)***	***E. coli*** ***A. index (%)***	***K. pneumonia*** ***A. index (%)***
$H_4[Cu_2(R^{2-})_2(R^-)_4]$	+64.28	+28.94	+53.57	+60.77
$H_8[Cu_2(R^{2-})_6en_2]$	+73.57	+25.26	+60.71	+76.92
$H_8[Cu_2(R^{2-})_6en]$	+52.14	+19.21	+46.42	+62.69
$H_4[Cu_2(R^{2-})_2(R^-)_4Ac_2]$	+10.71	-26.34	0.0	+50.0
$H_4[Cu_2(R^{2-})_2(R^-)_4enAc]$	-41.79	-43.16	-17.86	-21.92
$Na_8[Cu_2(R^{2-})_6]$	+28.57	-10.53	+25.0	+46.15

Note: (-) = lower antibacterial activity than the commercial antibiotic

(+) = higher antibacterial activity than the commercial antibiotic

4.4.1. Minimum inhibitory concentration

Minimum inhibitory concentration (MIC) is lowest concentration of an antimicrobial that will inhibit the visible growth of a microorganism following overnight incubation, usually reported as µg/mL or mg/L [**44**].The minimum inhibitory concentration (MIC) was determined by using a serial dilution method for selected complexes of $H_4[Cu_2(R^{2-})_2(R^-)_4]$ and $H_8[Cu_2(R^{2-})_6en]$ at100 mg/L, 300 mg/L, 500 mg/L and 700 mg/L concentrations against the four bacterial strains.

In this study the minimum inhibitory concentration of $H_4[Cu_2(R^{2-})_2(R^-)_4]$ for S. aurous and S.Pyogenes may be around 100 mg/l. But, for E. Coli and K. pneumonia may be around 300 mg/l see Table 8.

Table 8: MIC determination of selected $H_4[Cu_2(R^{2-})_2(R^-)_4]$ complex

Bacterial strains	**$H_4[Cu_2(R^{2-})_2(R^-)_4]$Concentration**			
	100 mg/L	300 mg/L	500 mg/L	700 mg/L
S. Aurous	-	-	-	-
S.Pyogenes	-	-	-	-
E. Coli	+	-	-	-
K. pneumonia	+	-	-	-

Note: (+): bacteria growth and (−): no bacteria growth.

According to the data the minimum inhibitory concentration of $H_8[Cu_2(R^{2-})_6en]$ for S.Pyogenes may be around 100 mg/l. But, for S. Aurous, E. Coli and K. pneumonia may be around 300 mg/l see Table 9.

Table 9: MIC determination of selected $H_8[Cu_2(R^{2-})_6en]$complex

Bacterial strains	**$H_8[Cu_2(R^{2-})_6en]$ Concentration**			
	100 mg/L	300 mg/L	500 mg/L	700 mg/L
S. Aurous	+	-	-	-
S.Pyogenes	-	-	-	-
E. Coli	+	-	-	-
K. pneumonia	+	-	-	-

Note: (+): bacteria growth and (−): no bacteria growth.

5. CONCLUSION AND RECOMMENDATION

5.1. Conclusion

In this study, novel homobinuclear complexes were synthesized, characterized and spuare planar and square pyramidal geometries around the metal center are proposed. The qualitative chloride test verified no ionizable chloride outside the coordination sphere. Besides, the pH values of the complexes revealed that they were acidic (Arrhenius type) in nature implying that the hydrogen ion acts as a counter ion except $Na_8[Cu_2(R^{2-})_6]$. According to the pH data, $Na_8[Cu_2(R^{2-})_6]$ is basic salt. The metal contents obtained experimentally, via ICP-OES after digesting the complexes in strong acid followed by dilution, agreed with the theoretical values of metal estimation. The observed shifts in band position and appearance of new non-ligand and ligand based bands in the UV-Vis spectra, IR spectra and cyclicvoltamogram confirmed the successful coordination of ligands to the metal center in the corresponding complexes. Generally, the information obtained from physicochemical, electrochemical and spectroscopic data supports the proposed structures of synthesized complexes.

Finally, the antibacterial screening and comparative study demonstrated that, all synthesized metal complexes except $H_4[Cu_2(R^{2-})_2(R^-)_4enAc]$ (from all tested bacteria) and $H_4[Cu_2(R^{2-})_2(R^-)_4Ac_2]$ (from S.pyogenes) exhibited higher antibacterial activity than the commercial antibiotic gentamycin. Therefore the complexes become potential alternative antibacterial drugs after their *in vivo* cytotoxicity, pre-clinical and clinical investigations.

5.2. Recommendation

Due to the limited availability of other spectroscopic techniques, the structures of newly synthesized mixed ligand complexes have been proposed only on the basis of physicochemical data, electrochemical data and spectroscopic data such as ICP-OES, UV-Visible, IR and CV. Hence the structure of complexes could be further studied with the advanced spectroscopic techniques such as X-ray crystallography, NMR, Mass spectroscopy and TGA.

The antibacterial activity of most of the synthesized complexes exhibited significant activity against all tested bacterial strains. So, the newly synthesized Cu (II) complexes could be further studied against many other bacterial and fungal strains. Besides, due to limited resources, the minimum inhibitory concentrations for all synthesized complexes were not determined.

Therefore, it could be done for all synthesized complexes with a closer concentration by considering this study as baseline information.

Since the *in vivo* activities of the complexes were not studied. So, the in vivo cytotoxicity investigation, pre-clinical and clinical tests must also conduct. After these, the newly synthesized complexes could be considered as potential antimicrobial agent.

6. REFERENCES

[1]. Golkar, Z., Bagasra, O., and Pace, D.G., 2014. Bacteriophage therapy: a potential solution for the antibiotic resistance crisis. *The Journal of Infection in Developing Countries*, 8, 129.

[2]. Li, B. and Webster, T.J., 2018. Bacteria antibiotic resistance: New challenges and opportunities for implant-associated orthopedic infections. *Journal of Orthopaedic Research*, 36, 22.

[3]. Tamiru, G., Abebe, A., Abebe, M. and Liyew, M., 2019. Synthesis, structural investigation and biological application of new mono-and binuclear cobalt (II) mixed-ligand complexes containing 1, 10-phenanthroline, acetamide and ethylenediamine. *Ethiopian Journal of Science and Technology*, 12, 69.

[4]. Gurumoorthy, P., Ravichandran, J. and Rahiman, A.K., 2014. Mixed-ligand binuclear copper (II) complex of 5-methylsalicylaldehyde and 2, 2′-bipyridyl: Synthesis, crystal structure, DNA binding and nuclease activity. *Journal of Chemical Sciences*, 126, 783.

[5]. Loganathan, R., Ramakrishnan, S., Suresh, E., Riyasdeen, A., Akbarsha, M.A. and Palaniandavar, M., 2012. Mixed ligand copper (II) complexes of N, N-bis (benzimidazol-2-ylmethyl) amine (BBA) with diimine co-ligands: efficient chemical nuclease and protease activities and cytotoxicity. *Inorganic Chemistry*, 51, 5512.

[6]. Shebl, M., El-ghamry, M.A., Khalil, S.M. and Kishk, M.A., 2014. Mono-and binuclear copper (II) complexes of new hydrazone ligands derived from 4, 6-diacetylresorcinol: Synthesis, spectral studies and antimicrobial activity. *SpectrochimicaActa Part A: Molecular and Biomolecular Spectroscopy*, 126, 232.

[7]. Kopel, P., Trávníček, Z., Marek, J., Korabik, M. and Mrozinski, J., 2003. Syntheses and properties of binuclear copper (II) mixed-ligand complexes involving thiodiglycolicacid.: The crystal structures of [(phen) 2Cu (μ-tdga) Cu (phen)]$(NO_3)_2 \cdot 5H_2O$ and [(H_2O)(pmdien) Cu (μ-tdga) Cu (pmdien)(H_2O)]$(ClO_4)_2$. *Polyhedron*, 22, 411.

[8]. Bayeh, Y., Abebe, A., Thomas, M. and Linert, W., 2019. Synthesis, Characterization and Antimicrobial Activities of New Mixed Ligand Complexes of Copper (II) with 1, 10-Phenanthroline and Thymine. *Journal of Transition Metal Complexes*, 2, 1.

[9]. Radalla, A.M., 2010. Studies on complexation of resorcinol with some divalent transition metal ions and aliphatic dicarboxylic acids in aqueous media. *Journal of Solution Chemistry*, 39,1394.

[10]. Samorodov, V.N., Pospelov, S.V., Moiseeva, G.F. and Sereda, A.V., 1996. Phytochemical composition and pharmacological properties of various species of the Echinaceamoench Genus (a review). *Pharmaceutical Chemistry Journal*, *30*, 245.

[11]. Paoletti, P., 1984. Formation of metal complexes with ethylenediamine: a critical survey of equilibrium constants, enthalpy and entropy values. *Pure and applied chemistry*, 56, 491.

[12]. Chohan, Z.H., Shad, H.A. and Supuran, C.T., 2012. Synthesis, characterization and biological studies of sulfonamide Schiff's bases and some of their metal derivatives. *Journal of Enzyme Inhibition and Medicinal Chemistry*, 27, 58.

[13]. Altundas, A., Sarı, N., Colak, N. and Ögütcü, H., 2010. Synthesis and biological activity of new cycloalkylthiophene-Schiff bases and their Cr (III) and Zn (II) complexes. *Medicinal Chemistry Research*, 19, 576.

[14]. Chen, G.J., Qiao, X., Qiao, P.Q., Xu, G.J., Xu, J.Y., Tian, J.L., Gu, W., Liu, X. and Yan, S.P., 2011. Synthesis, DNA binding, photo-induced DNA cleavage, cytotoxicity and apoptosis studies of copper (II) complexes. *Journal of Inorganic Biochemistry*, 105, 119.

[15]. Goo, Y.R., Maity, A.C., Cho, K.B., Lee, Y.M., Seo, M.S., Park, Y.J., Cho, J. and Nam, W., 2015. Tuning the reactivity of Chromium (III)-superoxo species by coordinating axial ligands. *Inorganic Chemistry*, 54, 10513.

[16]. Abebe, A. and Hailemariam, T., 2016. Synthesis and assessment of antibacterial activities of ruthenium (III) mixed ligand complexes containing 1, 10-phenanthroline and guanide. *Bioinorganic Chemistry and Applications* 2016, 1.

[17]. Wankhede, D.S., Mandawat, N.D. and Qureshi, A.H., 2014. Mixed ligand complexes derived from 4-(Benzene Azo) salicyladehyde and 2-amino-4-nitrophenol using transition metal ions. *Journal of Current Chemical Pharmaceutical Sciences*, 4,135.

[18]. Bodkhe, A.S., Patil, S.S. and Shaikh, M.M., 2012. Synthesis, characterization and antibacterial studies on mixed ligand copper complexes with polydentate ligands. *ActaPoloniaePharmaceutica*, 69, 871.

[19]. Angeluşiu, M.V., Almăjan, G.L., Ilieş, D.C., Roşu, T. and Negoiu, M., 2008. Cu (II) complexes with nitrogen-oxygen donor ligands: synthesis and biological activity. *Chem. Bull."Politehnica" Univ.(Timisoara)*, 53, 78.

[20]. Atanu, B., Sumana S, D. C., Enrique, C., and Kajal, K. R, 2008. Binuclear Copper (II) complexes with N_4O_3 coordinating heptadentate ligand: Synthesis, structure, magnetic

properties, Density-Functional Theory study, and catecholase activity. *Inorganic Chemistry*, 47, 4023.

[21]. Završnik, D., Muratović, S., Špirtović, S., Softić, D. and Medić-Šarić, M., 2008. The synthesis and antimicrobial activity of some 4-hydroxycoumarin derivatives. *Bosnian Journal of Basic Medical Sciences*, 8, 277.

[22]. Schmiedel, K.W. and Decker, D., 2000. Resorcinol. *Ullmann's Encyclopedia of Industrial Chemistry*.

[23]. Amirghofran, A.A., Rayatpisheh, S., Tanideh, N., Owji, A.A., Vasei, A. and Mehrabani, D., 2005. Evaluation of Different Formulations of Biological Surgical Adhesives on Hemorrhagic Aorta: An In vitro and Animal, Study. *Journal of Applied Animal Research*, 28, 121.

[24]. Thakur, U.K., Shah, D., Sharma, R.S., Sawant, R.M. and Ramakumar, K.L., 2006. Studies on protonation and Th (IV) complexation behaviour of dihydroxybenzenes in aqueous 1 M $NaClO_4$ medium. *Radiochimica Acta*, 94, 859.

[25]. Allen, P.W., Bowen, H.J.M., Sutton, L.E. and Bastiansen, O., 1952. The molecular structure of acetone. *Transactions of the Faraday Society*, *48*, 991.

[26]. Freeman, J.M., Kossoff, E.H. and Hartman, A.L., 2007. The ketogenic diet: one decade later. *Pediatrics*, 119, 535.

[27]. Driessen, W.L. and Groeneveld, W.L., 1969. Complexes with ligands containing the carbonyl group. Part I: Complexes with acetone of some divalent metals containing tetrachloro-ferrate (III) and-indate (III) anions. *Recueil des Travaux Chimiques des Pays-Bas*, 88, 977.

[28]. Gillespie, R.J. and Hartman, J.S., 1968. Nuclear magnetic resonance studies of ketone• BF3 complexes. II. The boron trifluoride catalyzed condensation of acetone. *Canadian Journal of Chemistry*, 46, 3799.

[29]. Joseph, P. and Blumenthal, W., 1959. Reactions of Zirconium tetrachloride with acetone. *The Journal of Organic Chemistry*, 24, 1371.

[30]. Krishna, P.M., Shankara, B.S. and Reddy, N.S., 2013. Synthesis, Characterization, and Biological Studies of Binuclear Copper (II) Complexes of (2E)-2-(2-Hydroxy-3-Methoxybenzylidene)-4N-Substituted Hydrazinecarbothioamides. *International Journal of Inorganic Chemistry*, 2013, 1.

[31]. Mokhtaruddin, N.S.M., Yusof, E.N.M., Ravoof, T.B., Tiekink, E.R., Veerakumarasivam, A. and Tahir, M.I.M., 2017. Unusual saccharin-N, O (carbonyl) coordination in mixed-ligand copper (II) complexes: Synthesis, X-ray crystallography and biological activity. *Journal of Molecular Structure*, 1139, 1.

[32]. Buchtík, R., Trávníček, Z. and Vančo, J., 2012. In vitro cytotoxicity, DNA cleavage and SOD-mimic activity of copper (II) mixed-ligand quinolinonato complexes. *Journal of Inorganic Biochemistry*, 116, 163.

[33]. Yi, N. Z., Ning Z., Peter, G. O., Yuan Z. Li, Wen B. C., and Mei J. W., 2002. Cyclic voltammetry characterization of metal complex imprinted polymer. *Journal of Molecular Recognition* 15, 204.

[34]. Misganaw, T., Alemayehu, Y., Negera, A., 2015. Assessment of Antibacterial Activities and Phytochemical Screening of Leaf and Fruit of Solanum Marginatum. *Journal of Biological and Chemical Research*, 32, 966.

[35]. Baraki, T. and Upadhyay, R.K., 2012. Synthesis Characterization and Antimicrobial Studies on Cr (III) Fe (II) and Co (II) Complexes of Ethylene Dianil of Ortho Hyroxyphenylglyoxal. *Doctoral dissertation, Haramaya University*.

[36]. D. Gürbüz1, A. Çinarli1, A. Tavman1 and A. Birteksöz., 2015. Synthesis, Characterization and Antimicrobial Activity of Some Transition Metal Complexes of *N*-(5-Chloro-2Hydroxyphenyl)-3- Methoxy-Salicylaldimine, *Chemical Society of Ethiopia*, 29, 63.

[37]. Bamfield, P., 1967. The reaction of cobalt halides with N-arylsalicylideneimines. *Journal of the Chemical Society A: Inorganic, Physical, Theoretical*, 804, 1.

[38]. Tümer, M., Köksal, H., Sener, M.K. and Serin, S., 1999. Antimicrobial activity studies of the binuclear metal complexes derived from tridentate Schiff base ligands. *Transition Metal Chemistry*, 24, 414.

[39]. Tenover, F.C., 2006. Mechanisms of antimicrobial resistance in bacteria. *The American journal of medicine*, 119, S3.

[40].Tweedy, B.G., 1964. Plant extracts with metal ions as potential antimicrobial agents. *Phytopathology*, 55, 910.

[41].Dharmaraj, N., Viswanathamurthi, P. and Natarajan, K., 2001. Ruthenium (II) complexes containing bidentate Schiff bases and their antifungal activity. *Transition Metal Chemistry*, 26, 105.

[42]. Lokhande, M.V. and Choudhary, M.R., 2014. Some transitional metal ions complexes with 3-{[(E)-(4-Fluorophenyl) Methylidene] amino} benzoic acid and its microbial activity. *International Journal of Pharmaceutical Sciences and Research*, 5, 1757.

[43]. Tanja, S.; Enisa, S.; and Braho, L.; 2016. Antibacterial activity of zinc(II) and copper(II) terpyridine complexes. *Second International Electronic Conference On Medicinal Chemistry,*1, 30.

[44]. Mousavi, M., Johari, B., Zargan, J., Haji Noor Mohammadi, A., Goudarzi, H.R., Dezianian, S. and KeshavarzAlikhani, H., 2019. Investigating Antibacterial Effects of Latrodectus Dahli Crude Venom on Escherichia coli, Staphylococcus aureus and Bacillus subtilis. *Medical Laboratory Journal*, 13, 14.

7. APPENDIXES

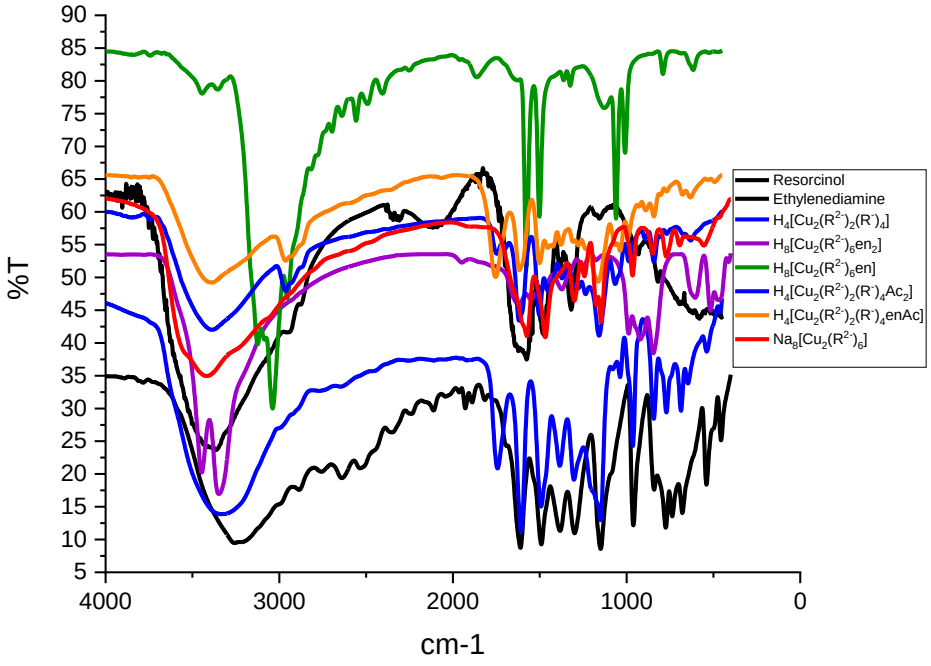

Appendix 1: The overlapped IR spectra of ligands and all synthesized complexes.

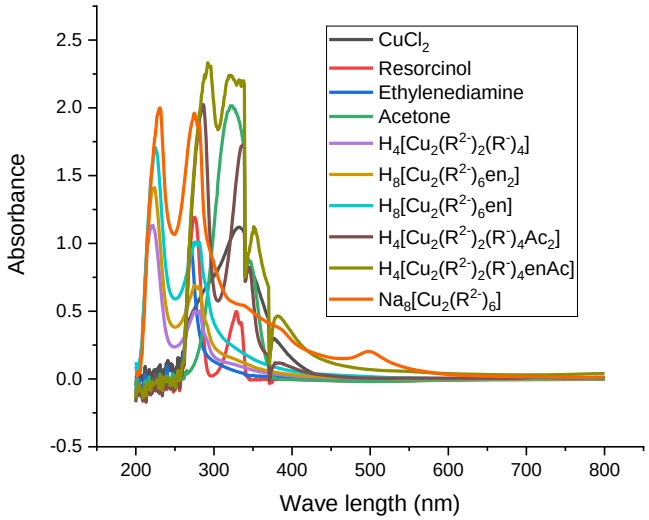

Appendix 2: The overlapped Uv-Visible spectra of $CuCl_2$, free ligands and all synthesized complexes.

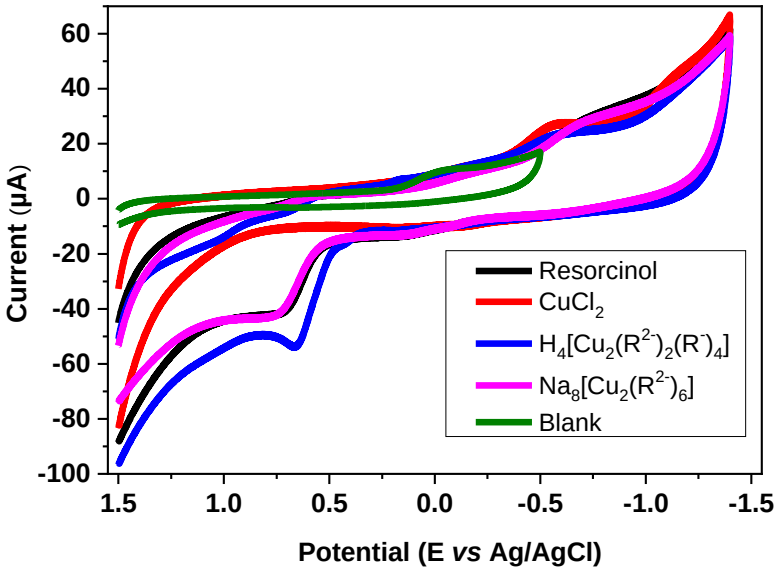

Appendix 3: Cyclicvoltamogram of $H_4[Cu_2(R^{2-})_2(R^{-})_4]$ and $Na_8[Cu_2(R^{2-})_6]$ with ligands and reference.

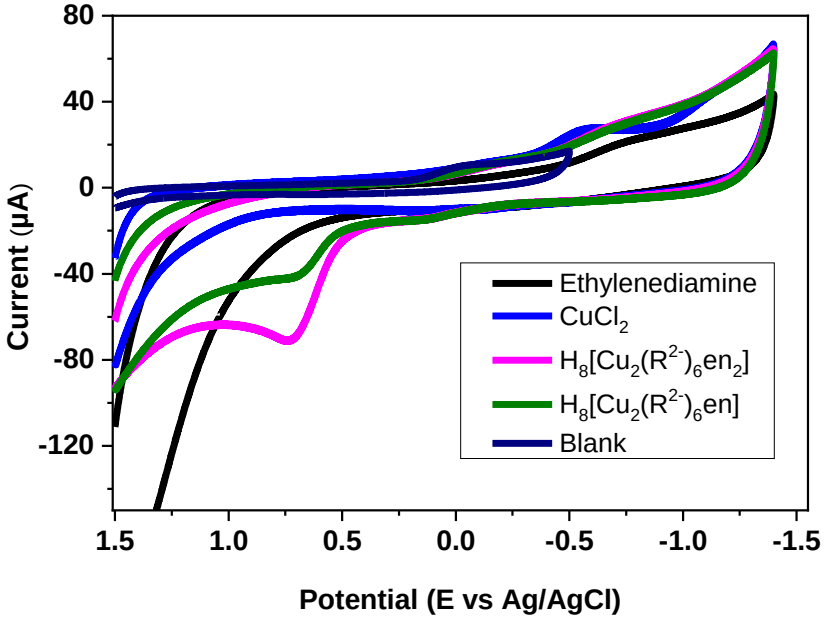

Appendix 4: Cyclicvoltamogram of $H_8[Cu_2(R^{2-})_6en_2]$ and $H_8[Cu_2(R^{2-})_6en]$ with ligands and reference.

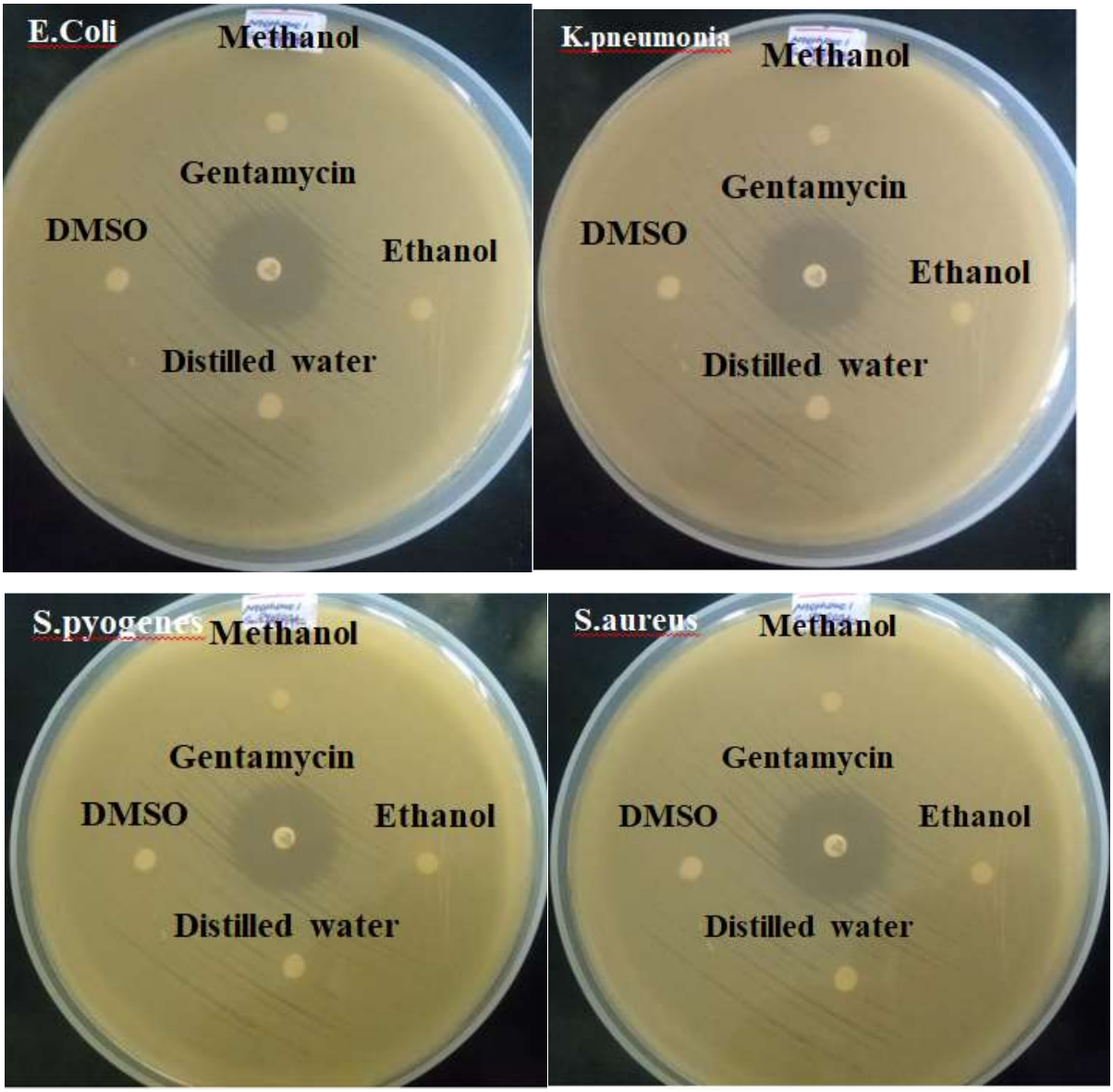

Appendix 5: Inhibition zone of the solvents used (Water and Ethanol) against two Gram-positive and two Gram-negative bacteria used for comparison.

Appendix 6: ICP-OES data of complexes obtained from measurement with respect to the standards.